NTNU

Untargeted analysis of DOM in an arctic fjord

Tobias Skaret Kielland

Department of Chemistry
Submission date: 01.07.2022
Supervisor: Murat V. Ardelan
Co-Supervisor: Maria Guadalupe Digernes
Faculty of Natural Sciences
Norwegian University of Science and Technology

1 Abstract

The Arctic Ocean is system that is quickly being altered due to climate change. Understanding the chemical properties of this region is essential in these times. In this study, the seasonal changes of dissolved organic matter (DOM) are looked at. The samples were taken in Ramfjoden at two stations, an inner and an outer, both with two depth, 5m and 30m. Furthermore the analysis was for done dissolved organic carbon(DOC) using an NPOC analyser and DOM was extracted using solid phase extraction and analysed with orbitrap mass spectroscopy. The DOC showed higher values in spring and autumn, with the highest being in spring, at 3.30mg/L. The DOM samples show distinct chemical changes happening in March, May, June and October. With tannin, protein and condensed aromatic -like compounds being the strongest indicators of this chemical change, while Lignin-like compounds were shown to be the larges fraction the compounds in the water column and a negative correlation with tannin. Over all this indicates a complex system of which a multitude of different factors such spring-bloom, melt water and other, alter the chemistry of the water column and provide the basis for marine life.

2 Preface

This thesis was done in the Environmental Chemistry and Toxicology (ENVI-TOX) program from the autumn semester 2020 until the spring semester 2022, in cooperation with a research project for Nansen legacy. And the publication will be delayed until the publication of that research project.

3 Acknowledgements

I would like thank Murat V ardelan for giving me the opportunity to do this project. and more so Maria Guadalupe Digernes for both giving me the opportunity, but also helping/guiding me with every aspect of the work.

I want to give a thanks to Yasemin Bodur, Martí Amargant-Arumí and Stephen Gustav Kohler for both helping me with lab work, as well as a special thanks to Yasemin and Marti for helping me with result interpretation and discussion.

I wanna thank Jeffrey Hawkes for provideing some of the matlab code used in the project and a big thanks to Håkon Espeland, Aase Mari Torseth and Nicholas Alexander Janjua for being supportive and helping various elements of the thesis.

Lastly i wanna thank Nicholas Alexander Janjua and Einar Falkeid for helping improve the grammar in the thesis.

Contents

4 Introduction

Dissolved organic matter (DOM) is on the worlds largest active reservoir of organic carbon at 662 GT[1]. this is approximately equivalent to the carbon stored in the atmosphere as CO_2[2]). This is a subject with large chemical complexity, affected by a huge number of biological and physical influences, such as warming, photosynthesis, heterotrophic microbial metabolism, and photochemistry. With this large complexity, the field of DOM is still underdeveloped.

being a reservoir of carbon in these times global warming means that the understanding of DOM has become critical. For both it's effect on the global carbon cycle[3], as well the climate effects a warming climate cause to the DOM.

DOM is defined as the fraction of organic compounds that can pass trough filter commonly 0.7μm, though big enough to be stopped by a smaller filter of 0.22μm. Dissolved organic carbon (DOC) is a closely related term that specifically referees only to the carbon in those compounds. This group of compounds contains reduce carbon, often bound to hetroatoms such as oxygen, nitrogen, phosphorus, and sulfur[4]. And provides the growth factors required for the metabolism of living-microbes, thus putting if at the base of the marine carbon cycle[4]. The biggest source of these compounds is the cellular material is released by metabolical activity from microorganisms. DOM may be released when cells die through processes such as viral lysis and predation by protozoa or bacteria.[5] However, DOM in itself is highly heterogeneous and complex Natural DOM mixtures, which comprises thousands of unique molecular masses, with numerous potential isomers at each mass[6].

5 List of Acronyms

Acronym	Full meaning
SPE	Solid phase extraction
C	Carbon
CO_2	Carbon dioxide
Cl	Chlorine
DOC	Dissolved organic carbon'
DOM	Dissolved organic matter
FT-ICR	Fourier transform ion cyclotron resonance
HTCO	High temperature catalytic oxidation
H	Hydrogen
N	Nitrogen
O	Oxygen
POC	Particulate organic matter
Pearsons test	Pearsons correlation coefficient test
P	Phosphorus
PCoA	Principal Coordinate Analysis
PC	Principal component
PCA	Principal component analysis
Se	Selenium
Na	Sodium
S	Sulfur
TOC	Total organic carbon
UiT	Universitet i Tromsø
13C	carbon thirteen
Go Flo	hydrostatic pressure activated sample bottles
m/z	mass to charge ratio
Aimod	modified armoticity index
NOM	natural organic matter
NDIR	non-dispersive infrared detector
NPOC	non-purgeable organic matter
QC	quality control
UP	ultra pure
MS	Mass spectrometry

6 Theory

6.1 Physical oceanic parameters

6.1.1 Fjords

A fjord is a deep, high latitude estuary, that have been excavated by a glacier[7]. They are often long, narrow and deep inlets, where the ice flow once followed a major fault. Fjords usually contain one or more submarine sills, which determine many of their distinctive physical and biogeochemical characteristics[7][8], fjords are efficient sediment traps because of these characteristics. Fjords function as a elongation of the sea inland and are thus strongly affected by mixing of fresh and seawater.[9]

The high latitude element of fjords makes it so that ice is an important element of a fjord altering the physical characteristics. These characteristics are the changing transmission of light through the water column and heat flux from the air to ocean. This will in turn alter biological conditions, such as increasing phytoplancton activitiy.[10] Another major seasonal change to a fjord is the circulation. Which changes from full vertical circulation to a two-layer circulation, creating high levels of water column stratification and a surface driven water discharge[11].

The Arctic Ocean is a system that has a significant input of terrestrial carbon. Which is mobilized from high latitude carbon-rich soils and peatlands[?]. which subsequently affects the fresh water discharge, the production of DOM in river catchments and the riverine transport of organic material input. Due to the large size of the DOM pool in inland waters, small changes to DOM mineralization and storage can cause large implications on global processes[6].

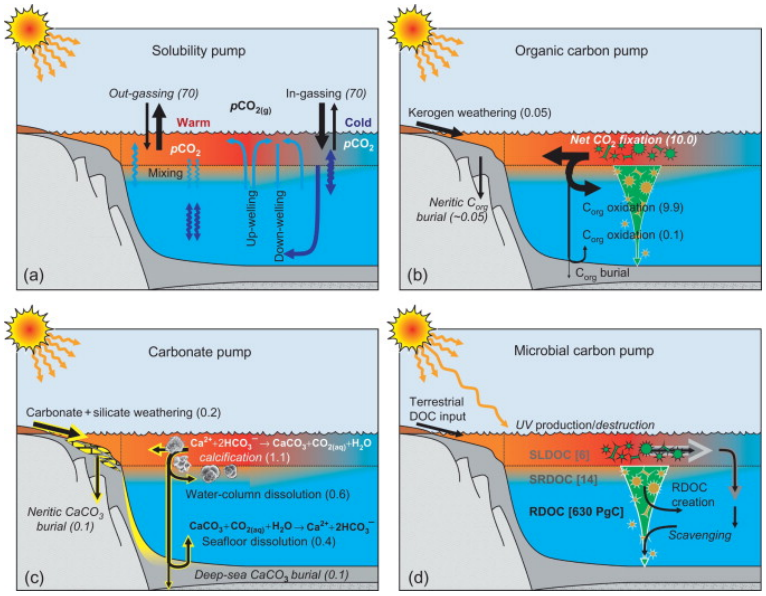

Figure 6.1: Schematic presentation of the different types of carbon pumps contribution to the oceans DOM. (a) The solubility. (b) The particulate organic carbon pump in the ocean. (c) The carbonate pump in the ocean. (d) The cycle of dissolved organic carbon in the ocean and the microbial carbon pump. [12] [14]

6.1.2 Carbon pumps

The biological pump is a process in which the sum of processes that transport photosynthetically-produced organic matter from the surface zone the of ocean to it's interior. This is done through combination of sinking particles, advection or vertical mixing of dissolved organic matter and transport by animals [1].

In the solubility atmospheric compounds like carbon dioxide (CO_2) drive the process, by dissolving into the ocean. This process is inversely correlated with the ocean temperature and as such the high latitudes oceans are the primary drivers, which cause the atmospheric carbon to go deeper through the thermo-haline circulation [12].

these processes move carbon from the surface layers of the ocean, down the water column, where carbon is dissolved and later converted to particulate form through primary production, which is then consumed by pelagic biota, exported to depth, and/or sequestered in the deep sea. [13]

The most intense increase of biomass DOM in a year, generally comes in the spring and is caused phytoplanktons. This phenomena is know as the spring bloom. In the time frame of this phenomena, there's up to a 100 times the

biomass turnover compared to plant based organic turnover. Followed by equally a fast consummation by grazers[15] [16]. This happens as a response to seasonal increases in temperature and solar radiation and event typically persists for a few weeks to months as nutrient limitation, cell sinking and grazing cause bloom collapse[17]. There's also been found evidence that a secondary similar biomass peak stimulated by excess nutrients can develop in late summer or autumn[17].

6.2 Instrumental

6.2.1 Solid phase extraction

Solid phase extractio (SPE) is a method that works by using the compounds physical and chemical properties to retain the wanted compounds within the extraction equipment. This is done by having surface of sorbent particles, with physical and chemical properties that make so that the compounds of interest are retained by adsorption, while the the rest is washed out by a solvent. The wanted compounds can later removed from the extraction equipment by using a stronger solvent and collected[18]. SPE has proved it's value in analytical research, but in the case of DOM has been found to only recover about 62% of DOC in salt-free extracts[19] and of this fraction the method was found to be better at retaining lignin and tannin like compounds, *especially compared to that of protein*.[20] [21].

SPE equipment used in DOM research is generally used specifically because of retention properties for organic molecules, which makes SPE useful for removing salt from the sample matrix, which is important not only for reducing matrix effect, but also salt potential damaging effects on sensitive ionization processes.[22] [23] Second, sufficient sample concentration can be required to ensure a suitable signal-to-noise ratio on the analytical equipment.[24]

6.2.2 Total organic carbon analysis

Total organic carbon (TOC) is a method used to look at total amount of carbon in a sample. This is done either by combustion or chemical oxidation[25]. One of these methods are High temperature catalytic oxidation (HTCO) which finds TOC by injecting the sample into a platinum catalyst at 680 °C in oxygen rich atmosphere and turned into CO_2. Where a carbon-free carrier gas transports the CO_2, through a moisture trap and halide scrubbers to remove water vapor and halides from the gas stream before it reaches the detector. the concentration of carbon dioxide generated is measured with a non-dispersive infrared detector (NDIR)[25].

6.2.3 Orbitrap Mass Spectrometry

Orbitrap Mass Spectrometry (orbitrap) is a mass analyzer where the ions created in the electrospray source are trapped in electrostatic fields, made from three electrodes. In the electrostatic field the ions start to oscillate based on their mass and emit current that is received by a image current detector. The strength of that current is applied Fourier transformation and two-point calibration to generate a mass spectrum[26] [27].

6.3 Elemental analysis

DOM is most commonly determined by the elemental components of its constituents, by looking at the distribution of the most common elements carbon (C), oxygen (O), hydrogen (H), nitrogen (N), sulfur (S), Phosphorus (P), Selenium (Se), Sodium (Na), Chlorine (Cl) and carbon thirteen (C13)[28]. This is determined by using each elements specified weight. C: 12 , O: 15.9949146, H: 1.007825 , N: 14.003074, S: 31.972071, P: 30.973762, Se: 79.916521, Na: 22.989770, Cl: 34.96885269 and C13: 13.00335. this only gives elemental composition, so to give a indication of the chemical structure of this formula the relative distribution of the set of compounds used[28].

Further insight for these compounds can be found by calculating the double-bond equivalentsy (DBE), which represents the sum of unsaturated rings in a molecule. calculated using the number of elements from the elemental distribution[29]:

$$DBE = 1 + \frac{1}{2}(2(C - O - N - S - P) - (H - N - P) + N + P) \tag{6.1}$$

Aromaticity index is another mathematical value commonly used. Which represents a threshold which indicates if a compound is aromatic. The two thresholds in DOM are AI$>$0.5 for aromatic compounds and AI$\geq$ 0.67 for condensed aromatic compounds[?].

$$AI = \frac{1 + C - O - S - 0.5H}{C - O - S - N - P} \tag{6.2}$$

6.3.1 Van Krevelen diagrams

Van Krevelen diagrams are commonly used in DOM research, for its ability to present large quantities of DOM. This diagram uses number of hydrogen divided by number of carbon carbon against number of oxygen divided by number of carbon, to visualize the diversity of compounds in a sample[30].

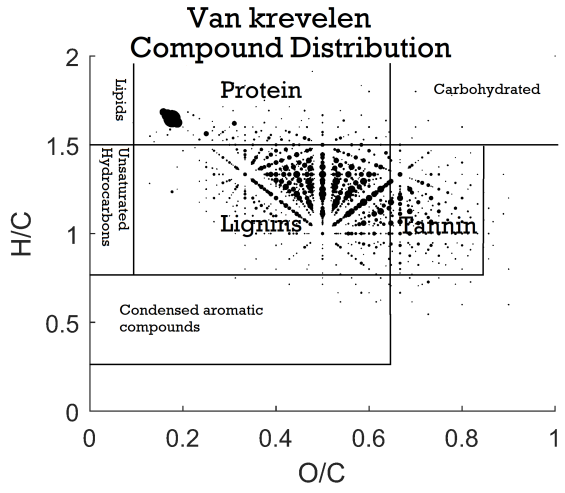

.

Figure 6.2: Visual representation of distribution of the divide of compound-like groupings within the Van Krevelen plot[31]. created by adding the shown boxes on top of the created Van krevelen plot show in figure 8.6

Further this method can be used separate the fingerprint data from the orbitrap into compound-like groups, which give a indication of how compounds with structures of that type or similar behave and behave in relation to each other. Although only if the relative fraction of these compounds is big enough[32][33].

Table 6.1: Ratios used to for the distribution of the FTICR finderprints, base on their ratios of O/C and H/C.[33]

Compound-like	O/C	H/C	N
Lipid	$0.01 \leq O/C \leq 0.1$	$1.5 \leq H/C \leq 2.0$	
Unsaturated hydrocarbon	$0.01 \leq O/C \leq 0.1$	$0.75 \leq H/C < 1.5$	
Condensed aromatic structures	$0.01 \leq O/C \leq 0.65$	$0.25 \leq H/C < 0.75$	
Protein	$0.1 < O/C \leq 0.65$	$1.5 \leq H/C \leq 2.3$	$N \geq 1$
Lignin	$0.1 < O/C \leq 0.65$	$0.75 \leq H/C < 1.5$	
Tannin	$0.65 < O/C \leq 0.85$	$0.75 \leq H/C \leq 1.5$	
Carbohydrate	$0.65 < O/C \leq 1.0$	$1.5 < H/C \leq 2.5$	

Lignin is together with cellulose and hemicellulose, one of the three biggest plant biomass components. It's a compound used in plants to make their plant structures rigid and protects against hydrolysis[34][35]. Lignin is in with this method generally one of the biggest fraction of the compound-like distribution. With the limited constraints of the method, a large amount of the compounds in this fraction are aromatic amines such as alkaloids, in addition to just lignins.[36][37] Lignin can come from terestial sources as well as oceanic Macrophyte or plants that have more complex structures. Benthic algae[38] was found to be made up of 50.6% lignin materials, followed by 17.4% tannins and 12.6% lipids and less defined structures[39].

Lipids are defined as the biological molecules readily soluble in organic solvents.[40] Algae-derived DOM contained greater proportions of lipids (56.8%), followed by lignin (15.0%) and protein (7.4%), but fewer tannins compared with macrophyte-derived DOM. The predominance of lipid compounds and absence of tannin formulas might therefore serve as an indicative feature of algae-derived DOM[41].

Tannins are water-soluble polymers capable of binding and/or precipitating water-soluble proteins[42].

Protein is a term that encapsulates a big variety of compounds that are connected by the fact that the are comprised of amino acids connected by peptides. Based on that definition a large number of the proteins exist within the constraints of the other compound-like groups and the protein fraction that is defined as protein like is more accurately described as peptides of 3 to 6 amino acid residues[36]. A typical indicatore of protein is phytoplankton, that is composed of 25–50% protein, 5–50% polysaccharide, 5–20% lipids, 3–20% pigments and 20% nucleic acids[43].

Carbohydrates are considered to be hexose and pentose glycosides, including those with aldehyde, ketone, and/or acid functionality[36].

Unsaturated hydrocarbon and *Condensed aromatic structures* are relatively small fractions based on this methodology, but in reality exist as bigger fractions that have been taken up by the other groups and as such are defined as the fraction of them self not contained in the other groups[36].

6.4 Statistics

6.4.1 Grubbs test

Grubbs test, also known as maximum normed residual test or “extreme studentized deviate test" is a test for detecting outliers. Where it detects an element as an outlier if that elements deviation from the mean is significant bigger then that of the standard deviation of the set. [44]

$$G = \frac{\max |Y_i - \bar{Y}|}{s} \tag{6.3}$$

Where G is grubbs value, s is standard deviation and $\bar{Y}$ is the sample mean.

6.4.2 Principal component analysis

Principal component analysis (PCA) is a method that used to reveal trends within a data set. It works by having the principal components (PC) orthogonal to each other and a reduction of the data is projected down to two dimensional or three dimensional space, where the eigenvalues of the variation are maximised [45] [46].

$$X = FQ^T = P\Delta Q^T \tag{6.4}$$

where:
X = The original data
F = The matrix of factor scores
Q^T = The transpose of the matrix of right singular vectors (tranposed matrix of loadings)
$P\Delta$ = the matrix of left singular vectors

PCs are attempts at understanding the underlying variation in the dataset. Some of the information is lost upon projecting into a low space and is represented by how much of variation remains in the PCs. IF the sum of variation in the PCs is low then 70% than PCA is considered unreliable.

The score plots represent a visualization of statistical similarity of the sample data. That are presented as points within the PC space. Each point is a sample and their relative position represent how similar are, within the parameters applied in the PCA.

Loadings plot represent a visualization of the weights for each variable within the PCA space. This presents the degree of collinearity among the variables and the relationship between how heavily each score is affected by each loadings. The plot is then visualized by the use of arrows in the PC space where each arrow is statistically more related to points and other arrows in it vicinity. This correlation comes from Pearson correlations[47].

Since PCA works by going through origo and can be heavily affected by the scale of the different factors, if the data does not center around origo then there is a need fore preprocessing. This can be done while scaling the factors magnitude to match each other, by subtracting every variable by it's mean and dividing each point by their standard deviation.[48]

$$z = \frac{x - \mu}{\sigma} \tag{6.5}$$

z = The processed score
x = The raw score
μ = the mean of the population
σ = the standard deviation of the population

This does not change the order of the observation of their relative distance, only the scale of the variables.

6.4.3 k-mean cluster

Clustering is a statistical method used to mathematically find samples that is similar in a data set. This is done by finding which samples are numerically closer to each other. Which can be done using k-mean clustering. This method finds centers in the data, where the mean of square euclidean distance is as low as possible.[49] This can be done together with other method such as PCA to find the samples that closest resemble each other in *created data.

Hierarchical clustering is another clustering method that instead creates clusters of 2 the points closest in space and then treats this clusters as a new single point,

repeating until every point within one cluster.

This method is further visualized by using dendrograms, which are graphic representations of the distance between the data. Where the x-axis contain the samples, with each having a vertical lines going. this turns 90°in the space, when these samples are considered a cluster by the hierarchical clustering method. As such the length of the vertical lines represent how clustered each samples is to another, which represents their similarity.[50]

6.4.4 Pearson's test

Pearsons correlation coefficient, also know as (Pearsons test) is a test used two differentiate between to data sets. The data sets are compared by fitting a line line through the data set and comparing slope of a fitted line. The growth rate of this slope is called coefficient R[51].

$$r = \frac{\sum_{i=1}^{n}(x_i - \bar{x})(y_i - \bar{y})}{\sqrt{\sum_{i=1}^{n}(x_i - \bar{x})^2}\sqrt{\sum_{i=1}^{n}(y_i - \bar{y})^2}} \tag{6.6}$$

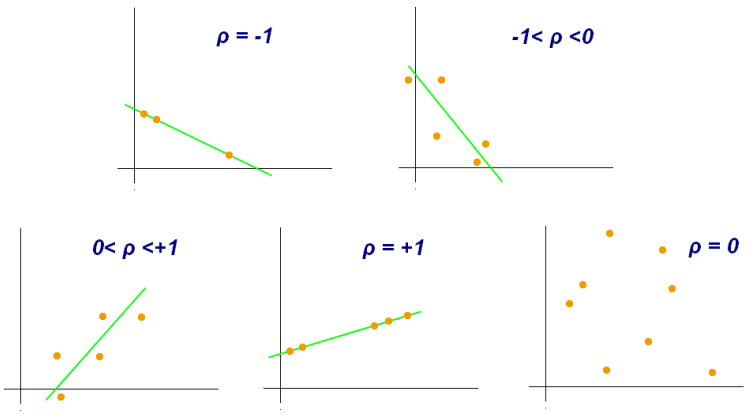

Figure 6.3: Example of Pearson's fitted line and its respective coefficient R, based on that line[52].

This coefficient ranges from -1 to 1 and the closer the values of the different set are, the more closely they correlate. This correlation is strengthened if the value is further away from 0. Represented as a strong positive correlation closer to 1 and strong negative correlation closer to -1[53]. That being said smaller sample size tend to have a higher frequency of R values closer to 1 and -1[54].

6.4.5 PCoA

Principal Coordinate Analysis (PCoA) is a method for measuring similarity (or dissimilarity) from pairs of objects and representing that similarity by showing the distances between points in a multidimensional space. this is done by mathematically or iteratively approximating the distance so that it's as close to the input distance, know as δ[55] [56].

$$\sigma(X) = \sum_{i=l}^{n} \sum_{j=l}^{n} w_{ij}(\delta_{ij} - d_{ij}(X))^2 \tag{6.7}$$

7 Method

7.1 Site description

Sample location was at Ramfjorden, in Finnmark, Norway (69°32'41.3"N 19°11'36.0"E), it's a fjord within the arctic circle. As such the inner part of the fjord freezes over in the winter. Blocking sampling at the inner station.[57] the fjord has 2 rivers running into it named Saltdalelva and Sørbotnelva, The samples were taken every month from September 2020 to august 2021 at the entrance of the fjord and at inner parts of the fjord, outline on 7.1. The sampling was done by lowering two hydrostatic pressure activated sample bottles (go-flo) to 5m and 30m respectively. The contents of the go-flow was then transfered to 3l nalgene bottles.

These bottles where then transferred to the University of Tromsø (UiT) where the filtration and extraction was done.

Figure 7.1: Sample stations in ramfjorden fjord. Made using google maps [58]

Figure 7.2: Picture of the fjord taken during sampling.

7.2 Filtration

All tubing and Nalgene bottles were rinsed with MQ water and then washed with 1% HCl by letting the items soak for at least 6 hours. items were then washed with MQ again, before being combusted for 5 hours at **°C. Plastic caps were washed by the same procedure but soaked for only 2 hours and disassembled prior to the wash. All glassware and filters were also combusted at 450°Cfor 5 hours.

The filtration was done in a room with only red light and temperatures at 8°C. Seawater was transferred to 1L amber Naglene bottles attached, via glass graduated pipettes, 5ml borosilicate, combusted (450°C, 5h). To a filtrations system of peristaltic silicone tubing (8 mm ID x 10 mm OD) on a Peristaltic pump (ISMATEC IPC high precision multichannel dispenser), at the end of the peristaltic pump were air filters were attached (Whatman, ReZist™, vwr, sterile, art. nr. 5140090, with precombusted 450°C GF/F filters, 0,7mm nominal pore size). The flow was run into waste desposial for 5min prior to sample collection to rinse the lines. The flowrate was set to <35mL/min and the collection was done in preweighed 40mL amber glass vials (pre-combusted and caps acid washed, Art. No. 23189. Sigma aldrich (Merck)), that then were acidified to 2pH using 8mL 6M ultra pure (UP) HCl (puriss p.a, ACS reagent), for DOC analysis and

Figure 7.3: Picture of the filtration setup, taken during the lab work

stored in the dark at 6°C. and in new preweighed 1L amber Naglene bottles for SPE-analysis.

7.3 Solid phase extraction

All vials and nalgene bottles and glass vials were pre-weighed on a μg weight. 1g SPE cartridges (Agilent Bond Elut PPL, 1g) were attached to a vacuum manifold and rinsed with 6mL >99,9% methanol and then filled with 3mL >99,9% methanol for it to soak in for 2 to 24 hours before the extraction.

The filtered water in the 1L Naglene bottles were acidified to 2pH, using 2.4ml 6M UP HCl. The bottles were attached with the same system of a peristaltic pump attached to the bottles, by attaching the tubing to glass graduated pipettes. Then* the extraction lies were run for 4mins at 3.5% flow rate equivalent to < 3ml/min to rinse. Every other month was run with blanks using the same Naglene bottles and method. The SPE cartridges were drained of MeOH and then added 6mL of 0.1% formic acid (VWR art. nr. 84865.180 (400 μl stock solution (50% formic acid) in 200 ml MQ with max 10ppb, before the SPE cartridges were drained of MeOH and attached to the end of the filtration system.

This system was then run until the 1L Naglene bottles were empty. At that point the SPE cartridges were detached and placed back on the vacuum manifold and rinsed with 6mL of 0.1% formic acid, before being purged with air for 10min by increasing the pressure on the manifold to less 5psi. The sample was then first eluted at gratiational flow, with 2mL 6M MeOH into 20mL precombusted 450°C vials and then with 4mL 6M MeOH, into seperate vials.

7.4 NPOC

The filtered 40mL vials were run for NPOC in a random order on the SHIMADZU TOC-V analyser. A calibration curve was made from a prepared standard solutions of 1, 2.5, 5, 10, and 100 ppm, that were run from 40ml vials at the start of the analysis. The filtrated samples where then run in groups of 8 followed by a quality control (QC). The QCs came from the same lab in Miami and had three different concentrations, representing low (41-43μM/L), mid (54-56 μM/L) and high (70-72 μM/L) water depth. These were run in a rotating order, each followed by a blank sample of MQ water and would be rerun with its 8 predecessors if detected value was outside 10% of their set values. This was done at the University of science and technology in Trondheim.

The method was validated using recovery samples. That were taken from the from the SPE samples. The samples had their methanol evaporated in an Ols aqua pro water bath and 30ml MQ water was added before the samples were run in the SHIMADZU TOC-V analyser. In the same way as the DOC samples.

7.5 Orbitrap MS

The SPE samples were run externally on a orbitrap mass analyzer at Uppsala univeristy, using the following procedure. Samples were diluted in 5% Acetonitrile solution. A 20μl sample was injected into an Agilent 1100 unit with a binary pump and a 100 x 2 mL well-plate autosampler with chromatographic column: Kinetex C18 column (2.1 x 150 mm, 2.6 μm bead size, 100 Å pore size). Two solvents were used, A) 18 MΩ deionized water + 0.1% formic acid and B) acetonitrile + 0.1% formic acid. A three step gradient was used where the initial flow rate was set to 150 μL $min^{-}1$. Secondly, at 10min the acetonitrile percentage was increased from 5 to 95% over 2 min and followed by a decrease to 5% at 12.10 min and held isocratic until 15 min. Lastly, the initial mobile phase composition was restored and maintained for 5 min until the next injection[59].

7.6 Digital treatment of data

The data was treated using Matlab and python. Matlab[60] was used to assign fingerprint compound formulae of chemical feasibility. Constraint to organic compounds, within the constraints of: O/C<1.2, H/C<2.25, H/C>0.3, N/C<0.5, S/C<0.2, (S+P)/C<0.2, DBE as a whole number and AImod[61]. Forward from here only samples with number of peaks over 1000 were used as samples under that value were to low in count to be considered accurate. Further matlab was used to create, with code provided by Jeffrey Hawkes, from Uppsala university. To plot the Van Krevelen diagrams and plotted 2d spectra from the orbitrap MS. Matlab was further used to apply Pearson test over the Van Krevelen. and then Van Krevelen diagrams containing only points with pearson test results over $\pm 0.5R$. PCoA and dendrogram were also plotted to show relationship between the overall distribution. using maximized euclidean distance and Hierarchical clustering respectively.

Python was used to create box and line plots using the matplotlib[62] package for the DOC samples. Outliers for these were removed using the grubbs outlier test, from the outliers package. Python was also used to assess the compound sub classes of the SPE samples[36][31]. These sub classes were normalized and analyzed using the Sklearns[63] PCA package. Both the barplots and the PCA for the compound-like groups, were plotted using matplotlib. Pandas[64] and numpy[65] was use in the data treatment to make the data applicable to the other packages.

8 Results

8.1 Instrumental work

As described in method the analytical instrument work part of the thesis was done externally in Uppsala university. The filtration and SPE was done at the University in Tromsø. The sampling was primarily carried out by members of a research group from Nansen Legacy and the time constrains when sampling, resulted in missing samples for the outer station April and sample being lost in transportation cause the loss of samples for August, from not being packed improperly. The sampling was done as close as to a month in between them.

8.2 NPOC

The full set of data from the NPOC runs are presented in appendix table 11.2. is that the DOC samples quality control samples never cause the sample runs to stop and the blank samples showed negative values, ranging from -0.11 to -0.25mg/L. This being below the calibration curve reduces the accuracy for those results. The accuracy of the calibration was check for, using blank samples that came with the calibration curve kit. These had much better result in the *-* range and were used for the rest of the samples, while the results with the old blanks were kept, as the range of value although negative, was small and in a small range. As the quality control samples were consistently within the accepted range.

The full values of the DOC samples are shown in appendix a table 11.2. This data has been shortened down to averages of all the samples at each samples point, with added minimum and maximum values, as well as number of samples in table 8.1.

Table 8.1: Table of average doc for each month at each station and depth. With their lowest, highest and average concentrations for the samples and number of samples from that point that were taken and were within the range the grubbs test. The outer station is labeled as S3 and the inner station is labeled as S1

month	avg conc(mg/L)	min conc(mg/L)	max conc(mg/L)	n-samples
JanS3 5m	1.100062	0.8186	1.547	8
FebS3 5m	1.8125	1.39	2.463	6
MarS3 5m	1.762143	1.099	3.356	7
AprS3 5m	2.6785	1.982	3.388	4
MayS3 5m	1.601	1.6	1.602	2
JunS3 5m	2.273857	2.046	2.573	7
JulS3 5m	1.5994	1.474	1.752	5
AugS3 5m	2.380667	1.533	3.173	6
SepS3 5m	1.556571	1.265	1.764	7
OctS3 5m	1.530143	1.152	1.83	7
NovS3 5m	1.038	1.029	1.047	2
DecS3 5m	1.0438	1.012	1.067	5
JanS3 30m	1.043243	0.8142	1.294	7
FebS3 30m	1.95545	0.9658	3.624	6
MarS3 30m	1.742667	1.24	2.686	6
MayS3 30m	3.307167	2.643	3.973	6
JunS3 30m	1.71375	1.231	2.202	4
JulS3 30m	1.706	1.705	1.707	2
AugS3 30m	1.367571	1.095	1.531	7
OctS3 30m	1.356429	1.143	1.76	7
NovS3 30m	2.0985	1.603	2.594	4
DecS3 30m	1.061057	0.9425	1.182	7
SepS1 5m	2.158	1.378	2.668	7
OctS1 5m	2.253667	1.32	2.975	6
NovS1 5m	1.964	1.273	2.653	4
JulS1 30m	1.44175	1.232	1.653	4
SepS1 30m	2.408167	1.581	3.088	6
OctS1 30m	2.625714	1.902	3.521	7
NovS1 30m	1.620514	0.9118	2.497	7

Figure 8.1 was made by plotting the average concentration of DOC for each month, with matplotlib. Plotted separately for each combination of depth and position in the fjord. Grubbs test was applied with an alpha value of 5, to full range of samples before the average values were calculated. Further the inner station only has samples from the dates where the inner parts of the fjord was ice free.

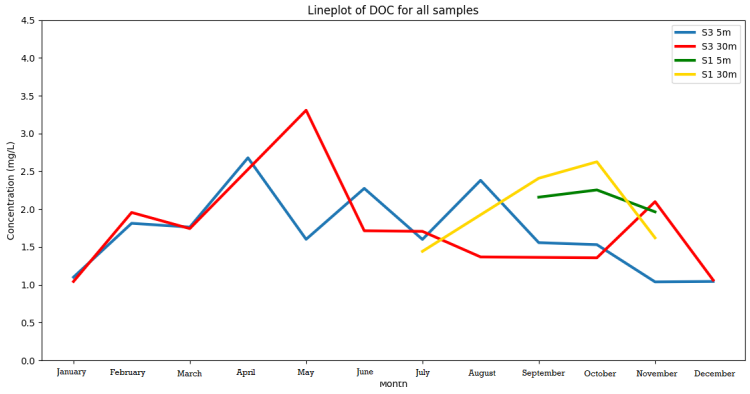

Figure 8.1: Lineplot showing the average concentration of DOC for all the samples found by looking at their NPOC values and divided based on their depth and location

Variance of each of the lineplots in figure 8.1 are plotted for each station in figure 8.2, figure 8.3, figure 8.4 and figure 8.5. Each lineplot of the average concentration was calculated in the same way as figure 8.1. The variance in each samples was applied on top as boxplots, showing the range of which 50% of the sample concentration values are concentrated and the median of each sample group is visualized as as an orange line in the boxplots.

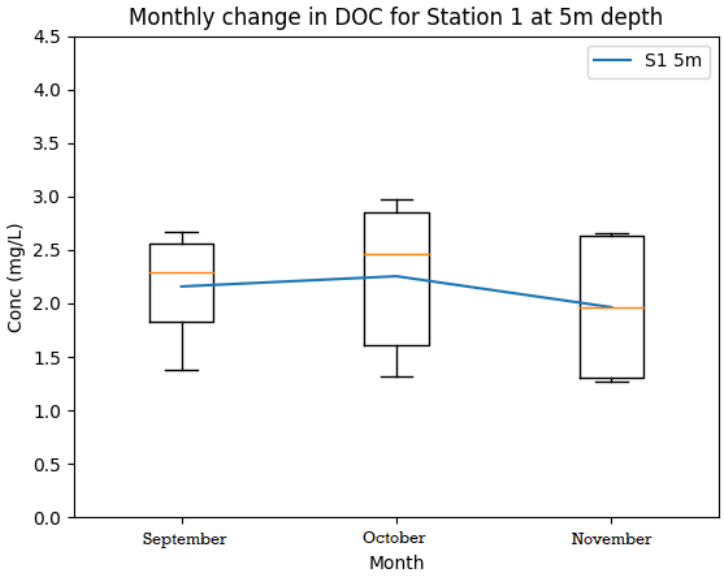

Figure 8.2: Lineplot of the samples at the inner station and 5m depth, found by measuring the samples NPOC. Showing the change in average concentration, with added boxplot representing 50% of the DOC of each sampling month and the median of the samples as an orange line.

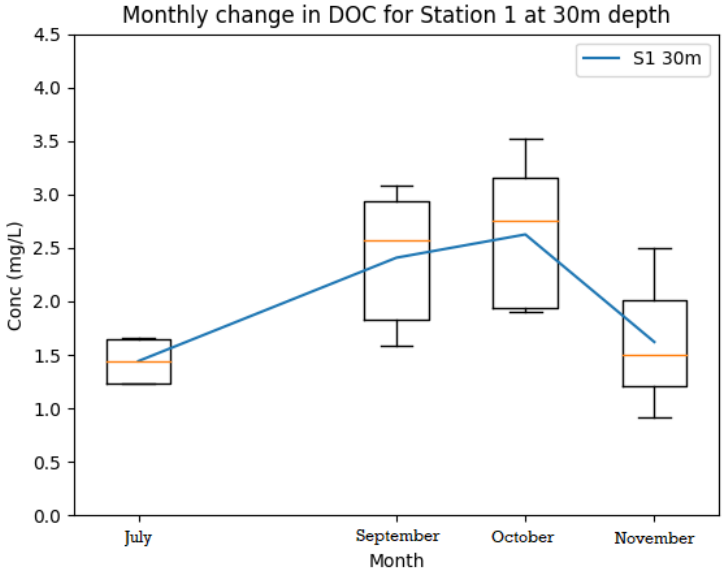

Figure 8.3: Lineplot of the samples at the inner station and 30m depth, found by measuring the samples NPO. Showing the change in average concentration, with added boxplot representing 50% of the DOC of each sampling month and the median of the samples as an orange line.

The range of the inner 30m in figure 8.3 is quite limiting for these samples, that being said the variance is quite low so strengthening the accuracy. Even if it's only showing a linear trend of limited change. The July samples were deemed as outliers by the Grubbs test and have values ten fold the average and as such are likely contaminated. Unfortunately limiting the ability to compare with the 30m samples.

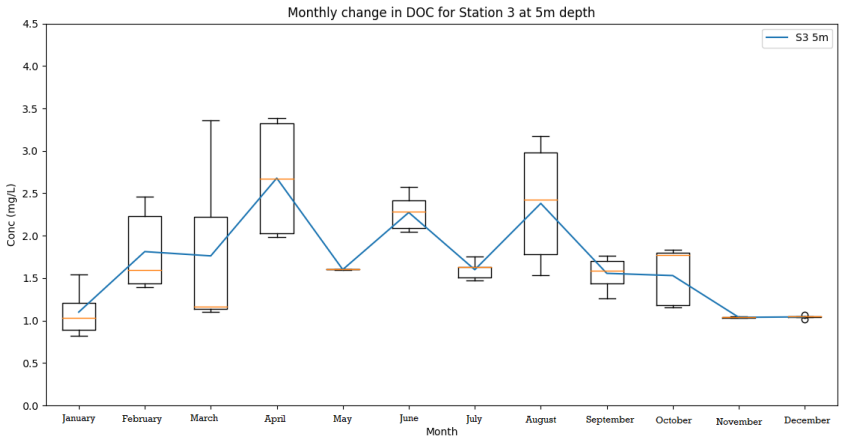

Figure 8.4: Lineplot of the samples at the outer station and 5m depth, found by measuring the samples NPO. Showing the change in average concentration, with added boxplot representing 50% of the DOC of each sampling month and the median of the samples as an orange line.

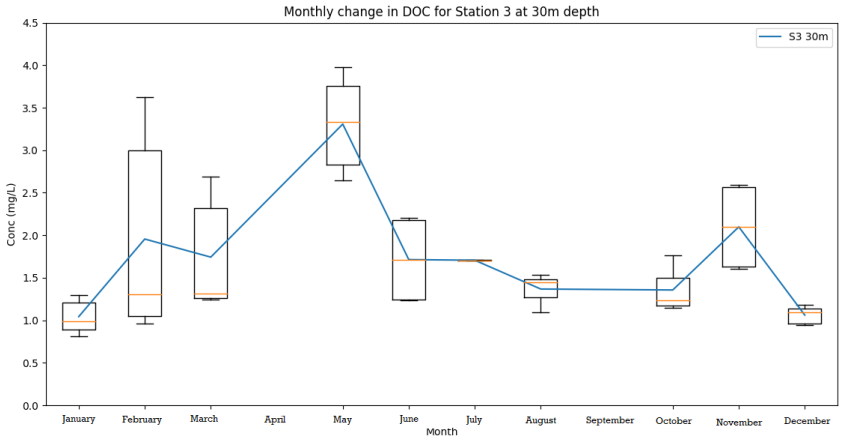

Figure 8.5: Lineplot of the samples at the outer station and 30m depth, found by measuring the samples NPO. Showing the change in average concentration, with added boxplot representing 50% of the DOC of each sampling month and the median of the samples as an orange line.

Using the trends show in figure 8.1 the general trend for the outer samples is a overall growth towards springtime, peaking earlier for the 5m samples in April (2.6785mg/L) and May for the 30m samples (3.307167mg/L). Taking the integral of curves from the outer station gives the 5m samples 20,377mg/L, figure 8.4 and the 30m samples 19.877mg/L, figure 8.5. Showing that over the course of the whole time series, that for the outer station the concentration of the 5m samples were higher.

Both the 5 and 30m samples of the inner station, from figure 8.2 and figure 8.3, show a small variance between samples averages and within the samples of each month. With both having the highest range in October 1,655mg/L and 1.619mg/L respectively. The 5m depth samples show a linear trend, while the 30m depth samples curve with a clear peak in October.

8.3 Solid phase extraction

The SPE samples that were run through the orbitrap were assigned fingerprint elemental values, and the hydrogen and oxygen values were divided by the carbon values for each compound, to create a Van Krevelen scatter plots for each samples, shown in figure 8.6 for the September inner station at 5m depth.

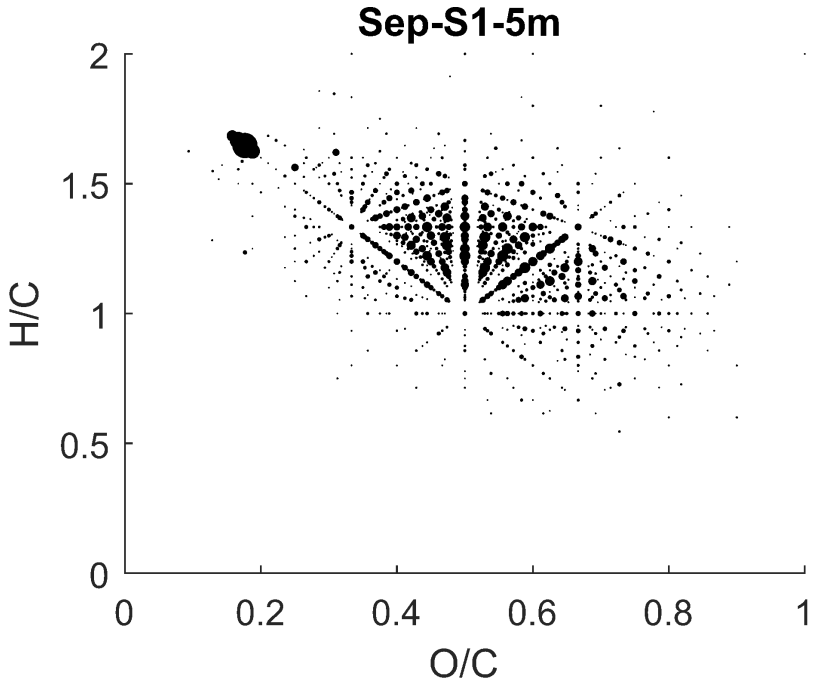

Figure 8.6: Van Krevelen scatter plot of H/C and O/C values from the peaks in orbitrap. Run of the september inner station at 5m depth.

The averages of these values are presented in table 8.2, with their respective number of peaks and the average of these samples aromacicity index.

Table 8.2: Table of orbitrap samples, with their respective number of peaks and their average hydrogen to carbon ratio, oxygen to carbon ratio aromacicity index

Sample name	number of peaks	average H/C	average O/C	average Aromacicity index
Sep S1 5m	1180	1.297640	0.494205	366.293152
Sep S1 30m	1135	1.271079	0.508939	372.653579
Sep S3 5m	1139	1.256605	0.505621	372.196560
Oct S1 5m	1124	1.285429	0.499586	364.165872
Oct S1 30m	1367	1.288663	0.504233	368.702865
Oct S3 5m	1516	1.279116	0.504227	365.759110
Oct S3 30m	1299	1.283622	0.506544	368.086053
Nov S1 5m	1410	1.274905	0.514773	375.593801
Nov S1 30m	1505	1.287034	0.503629	371.581898
Nov S3 5m	1277	1.293083	0.504374	375.295292
Dec S3 5m	1504	1.279985	0.508207	367.231966
Jan S3 5m A	1245	1.276946	0.515539	366.561322
Jan S3 5m B	1493	1.298659	0.506703	365.503656
Jan S3 5m C	1434	1.283394	0.518803	368.413417
Jan S3 30m	1395	1.291072	0.509665	366.731172
Feb S3 5m	1287	1.280538	0.509184	368.542003
Feb S3 30m	1335	1.287926	0.495098	367.110071
Mar S3 5m A	1353	1.295260	0.497683	369.847081
Mar S3 5m B	1050	1.309327	0.498437	368.614205
Mar S3 5m C	1232	1.314687	0.500438	375.212575
Mar S3 30m	1133	1.317831	0.498874	370.734416
apr S3 5m	1605	1.273765	0.511864	369.345143
apr S3 30m	1314	1.285892	0.504842	370.053873
may S3 5m A	1476	1.285114	0.503478	367.399745
may S3 5m B	1001	1.318704	0.490393	371.907977
may S3 5m C	1084	1.297146	0.501536	369.092247
may S3 30m	1522	1.293967	0.496307	368.361209
jun S3 5m	1252	1.247829	0.508711	367.607096
jun S3 30m	1240	1.278051	0.501437	374.995856
jul S1 5m	585	1.335659	0.499849	376.098933
jul S1 30m	639	1.298421	0.492836	366.754891
jul S3 5m	211	1.394944	0.452531	390.738175
jul S3 30m A	223	1.370956	0.440158	397.889309
jul S3 30m B	543	1.298357	0.492655	368.126393
jul S3 30m C	581	1.377588	0.476226	372.714602

Table 8.2 shows that the average values of hydrogen and oxygen to carbon ratios remain fairly stable throughout the whole time series. Same goes for the average aromacicity. The number of peaks also show that July had peak counts in to low of a value to be used in the statistics. This was most likely cause by there being problems with the elution, where as the solvent completely leave the SPE cartridge at a normal pace and as such the were likely some mistake either in the equipment or the lab work.

Ice was also found in SPE samples from march to July which indicates that formic acid wasn't completely purged from the SPE cartidges.

The evaluation of the method is presented graphically as recoveries in 8.7 and as a percentage fraction in table 8.3. The recovery samples are taken from the SPE samples and run as NPOC samples.

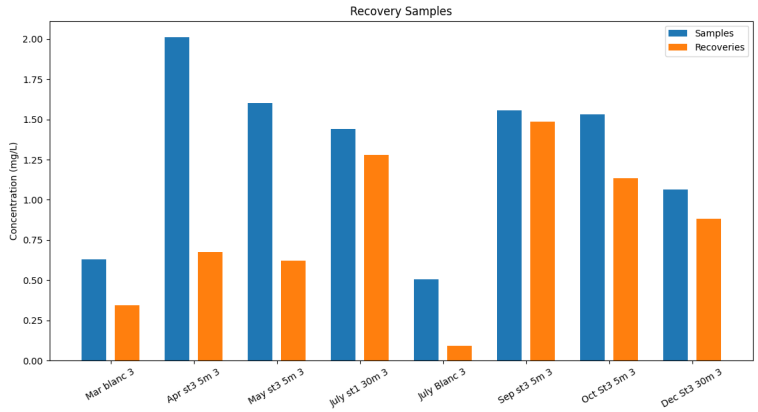

Figure 8.7: Graphical presented concentration of recovery samples, next to their counterpart DOC samples, based on their NPOC results.

Table 8.3: Recovery samples as their percentage of recovered concentration. Taken from the SPE samples and run as NPOC after methanol evaporation and MQ water addition. Recovered amount i calculated from the recovery sample concentration devide by their respective DOC sample concentrations

Sample	Recovery (%)
March blank 3	54.49
April Station 3 5m	33.62
May Station 3 5m	38.88
July Station 1 30m	88.82
July Blank 3	17.91
September Station 3 5m	95.39
October Station 3 5m	74.22
December St 3 30m	82.82

8.4 Statistics

8.4.1 Non-distributed statistics

Moving on to the statistics. The samples with a number of peaks less then 1000 and containing peaks removed by Grubbs test with an alpha value of 0.005, were deemed to be outlier and not used in the statistical analysis. The full set of sample with over 1000 peaks at the outer station are presented in figure 8.8 as a combined Van Krevelen plot. Where every compound has been run through Pearson's test and is outputted onto the plot, as a colour ranging from blue to yellow (-1R to 1R). presented next to a PCoA made from the orbitrap assigned elemental values and their peak size, with the individual samples number of peaks added on top of the plot as colour. Followed by plots where only the values furthest away from the extremes are filtered out.

These values were further interpreted using k-mean clustering to create dendrogram and a heatmap matrix shown in figure 8.9

And the method was applied to the sample at 5m and 30m depth. Creating figure 8.10 and figure 8.12 respectively, for the pearsons test and figure 8.11 and figure 8.13 for the dendrogram.

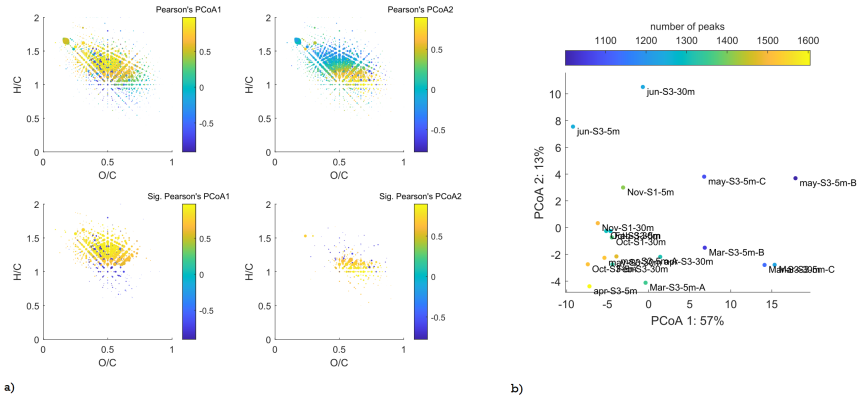

Figure 8.8: Figure a) Pearsons test overlayed the sum of the Van krevelen plots from the outer station
Figure b) PCoA plot for the samples from the outer station. Made from the orbitrap assigned elemental values and their peak size, with the individual samples number of peaks added on top of the plot as colour.

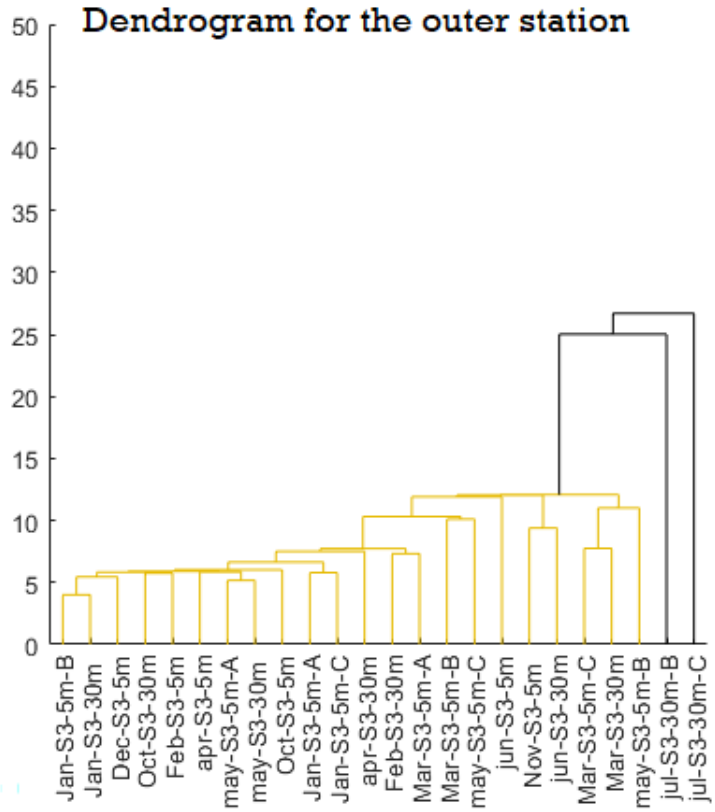

Figure 8.9: Dendrogram for clustering in the PCoA 8.8. Showing the level of similarity between samples at the outer station

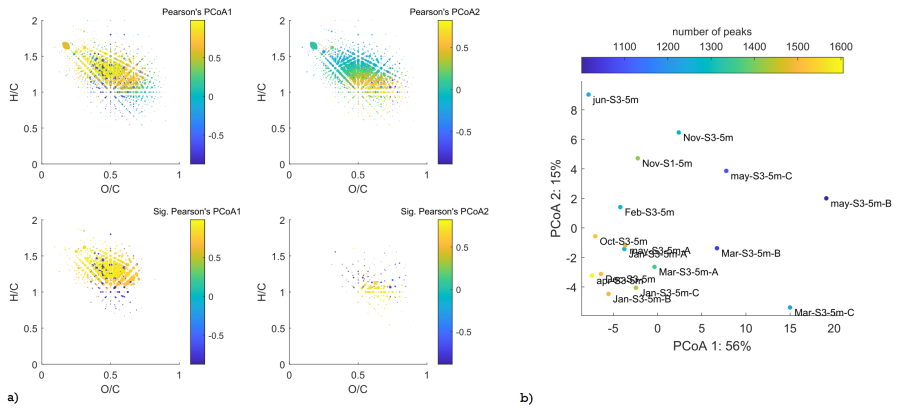

Figure 8.10: Figure a) Pearsons test overlayed the sum of the Van krevelen plots for all the samples at 5m depth
Figure b) PCoA plot for all the samples at 5m depth. Made from the orbitrap assigned elemental values and their peak size, with the individual samples number of peaks added on top of the plot as colour.

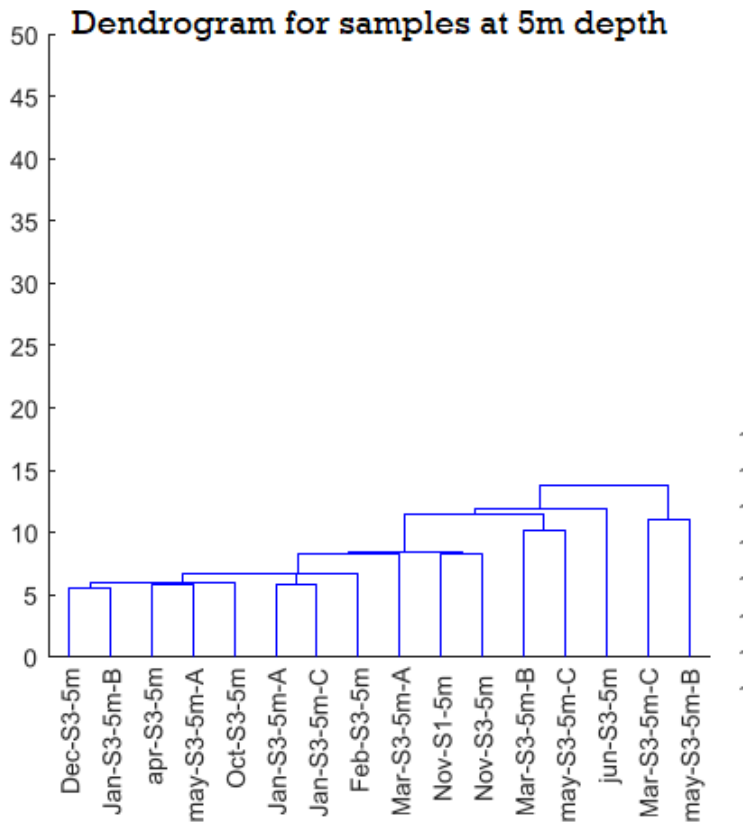

Figure 8.11: Dendrogram for clustering in the PCoA 8.10. Showing the level of similarity between samples at a depth of 5m

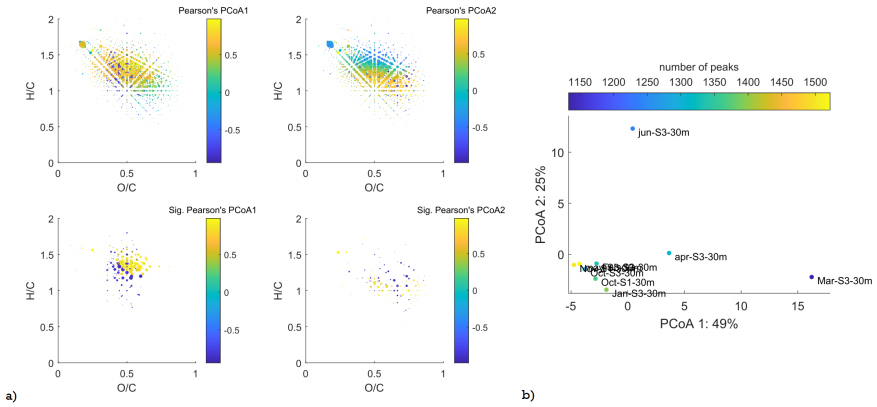

Figure 8.12: Figure a) Pearsons test overlaid the sum of the Van krevelen plots for all the samples at 30m depth
Figure b) PCoA plot for all the samples at 30m depth. Made from the orbitrap assigned elemental values and their peak size, with the individual samples number of peaks added on top of the plot as colour.

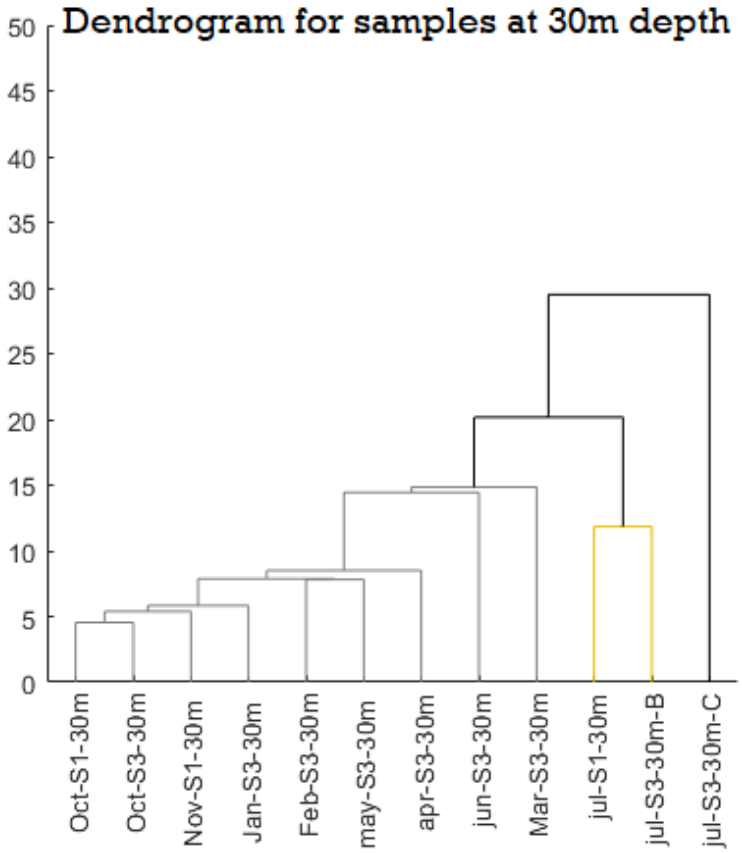

Figure 8.13: Dendrogram for clustering in the PCoA 8.12. Showing the level of similarity between samples at a depth of 30m

Rounding out these plots, the full range of samples have also gotten and also applied to all samples shown in figure 8.14 for Pearsons test and PCoA and figure 8.15 for the dendrogram.

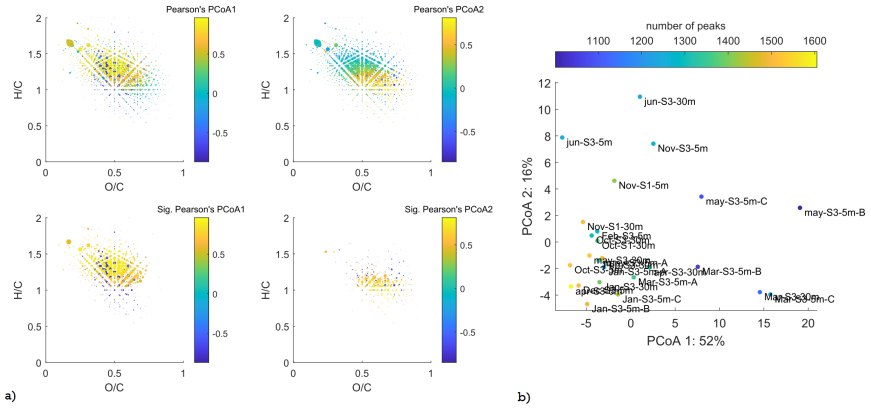

Figure 8.14: Figure a) Pearsons test overlaid the sum of the Van krevelen plots for all samples. Figure b) PCoA plot for all samples. Made from the orbitrap assigned elemental values and their peak size, with the individual samples number of peaks added on top of the plot as colour.

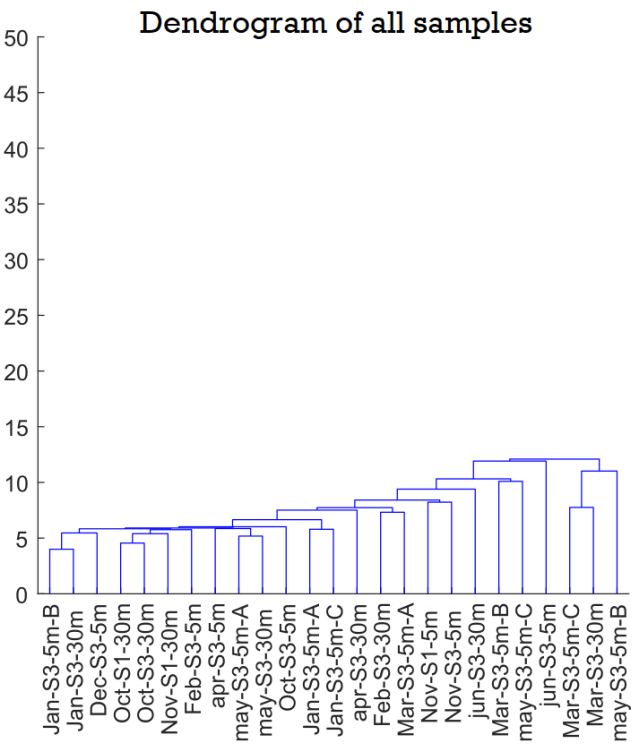

Figure 8.15: Dendrogram for clustering in the PCoA 8.14. Showing the level of similarity between all the samples.

For the plots overlaid the van krevelen plots figures8.12, 8.10, 8.8 and 8.14. Show there's a clear clustering in the full set of samples, in a region around 1H/C and 0.5O/C. Much like that of single sample, figure 8.6. this area in the area that's are more lignin/protein-like.

Further more, there's a distinct major peak in the top left of the plot, but this point is seemingly remain fairly unchanged trough out the time series, as it's pearsons values isn't high enough to get through the pearsons filter.

Looking only at the 5m PCoA in figure 8.8, there's a major distinction between the samples from May, March and June compared to the rest of the samples. Is most predominated by the may samples, based on the significance of the PCoAs

The same general trends that were seen when looking at the outer samples as a whole can also been seen here. Although with November as outliers in the full PCoA and a significantly lower count on the peaks in PCoA2.

Looking at the 30m Pearson values in figure 8.12 there's more of a significant change. In the significant Pearsons values there's a shift towards a narrower part of the Van Krevelen diagram on the O/C axis and a significant drop of these peaks in the parts of the diagram with higher H/C values

8.4.2 Compound-like distribution

using the fingerprint compound-like grouping to filter the peaks into compound-like groupings, the data of the orbitrap was used to create distributions of the total peak area of these compounds. These are shown as barplots in figure 8.16 and figure 8.17 for compound of the inner station at 5m and 30m depth. These are accompanied by barplots of the relative percentage of each compound compared to the rest of the compounds. The plots were predominantly lignin and tannin and as such are followed by a plot where these compound groups, are removed in figure 8.18.

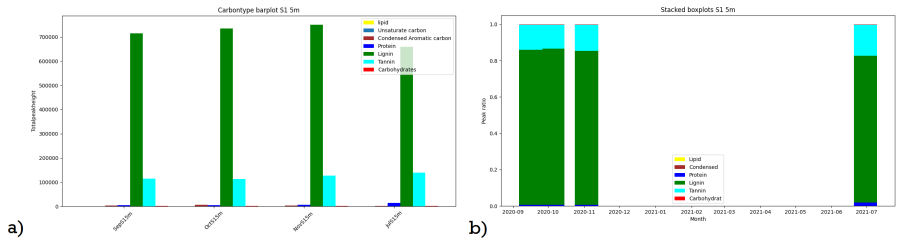

Figure 8.16: Figure a) Barplot showing the total peak area of different compound groups based on their H/C and O/C values at the inner station at 5m depth.
Figure b) barplot showing the relative size of the different compound groups in relation to each other at the inner station at 5m depth.

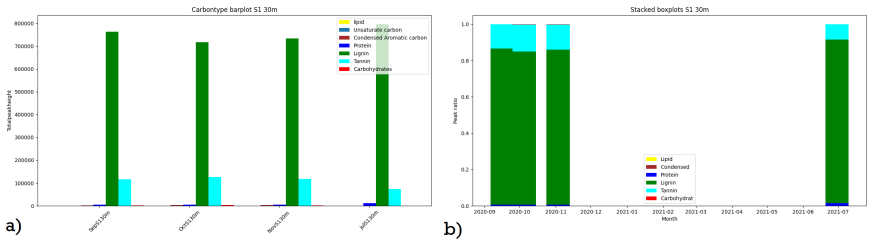

Figure 8.17: Figure a) Barplot showing the total peak area of different compound groups based on their H/C and O/C values at the inner station at 30m depth.
Figure b) barplot showing the relative size of the different compound groups in relation to each other at the inner station at 30m depth.

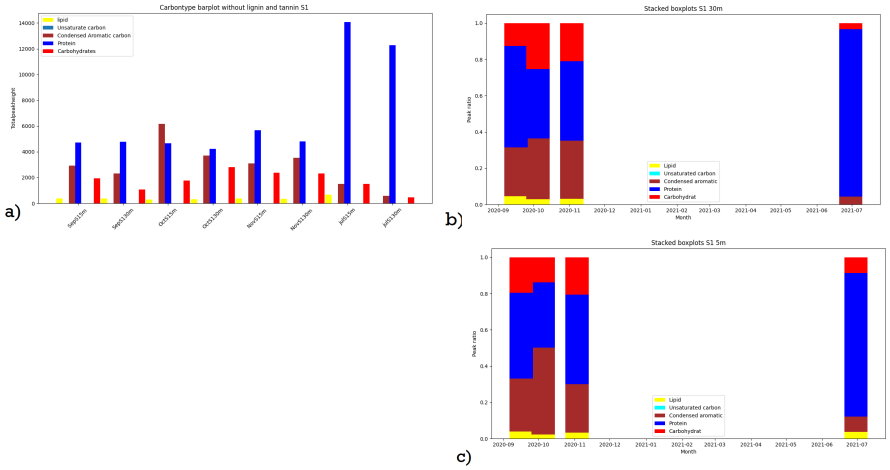

Figure 8.18: Figure a) Barplot showing the total peak area of different compound groups based on their H/C and O/C values at the inner station. Without the two biggest compound groups (Tannin and Lignin).
Figure b) barplot showing the relative size of the different compounds in relation to each other, at the inner station. Without the two biggest compound groups (Tannin and Lignin).

This method has further been added to the 5m and 30m depth samples of the outer station to create figure 8.19 and 8.21. these are also follow by plots without tannin and lignin in figure 8.20 and figure 8.22.

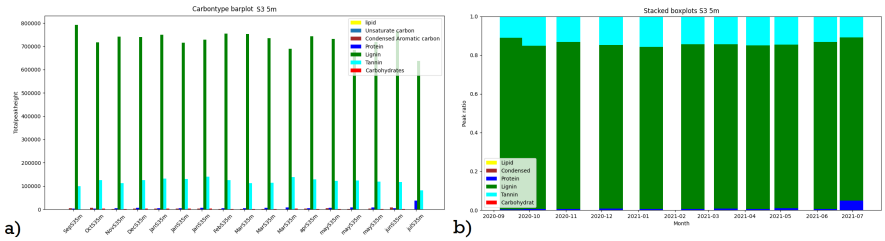

Figure 8.19: Figure a) Barplot showing the total peak area of different compound groups based on their H/C and O/C values, at 5m depth and the outer station.
Figure b) barplot showing the relative size of the different compound groups in relation to each other, at 5m depth and the outer station.

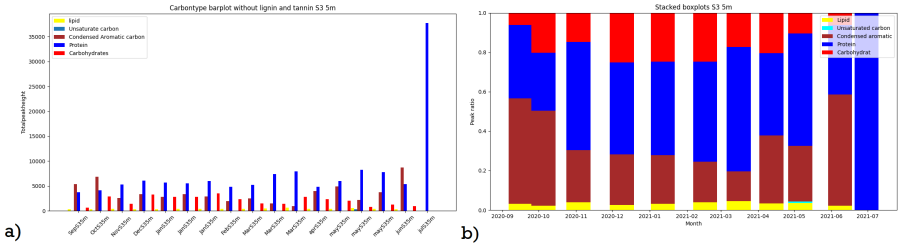

Figure 8.20: Figure a) Barplot showing the total peak area of different compound groups based on their H/C and O/C values at 5m depth and the outer station. Without the two biggest compound groups (Tannin and Lignin).
Figure b) barplot showing the relative size of the different compounds in relation to each other, at 5m depth and the outer station. Without the two biggest compound groups (Tannin and Lignin).

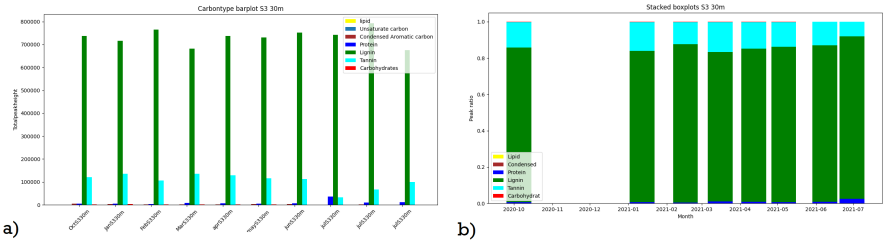

Figure 8.21: Figure a) Barplot showing the total peak area of different compound groups based on their H/C and O/C values at 30m depth and the outer station.
Figure b) barplot showing the relative size of the different compound groups in relation to each other, at 30m depth and the outer station.

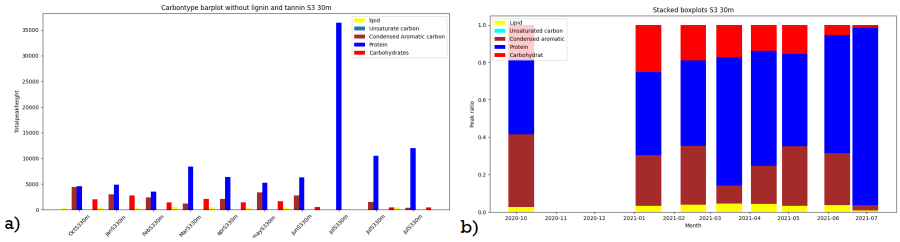

Figure 8.22: Figure a) Barplot showing the total peak area of different compound groups based on their H/C and O/C values at 30m depth and the outer station. Without the two biggest compound groups (Tannin and Lignin).
Figure b) barplot showing the relative size of the different compounds in relation to each other, at 30m depth and the outer station. Without the two biggest compound groups (Tannin and Lignin).

The distribution is over all predominated by the lignin-like fraction, Containing 84,2%(inner 5m), 86,1%(inner 30m), 85,1%(outer 5m) and 84,9%(outer 30m) of the distribution. This can also be seen as the middle of the cluster in figure 8.6. Tannin which follows as the second biggest in the range of 14,3%(inner 5m), 12,7%(inner 30m), 13,6%(outer 5m) and 13,7%(outer 30m). Looking within the compound-like fractions. the relative variance of the protein, tannin and condensed aromatic structures are the highest, with protein largest of those at at 0,0024%(inner 5m), 0,0035%(inner 30m), 0,034%(outer 5m) and 0,0076%(outer 30m). the full range of values are shown in table **??** in appendix a.

Meanwhile condensed aromatic carbon showed the greatest relative difference between depths, with an average of 0.0043m/z at 5m and 0.0030m/z at 30m or 70% less from 5 to 30m.

In an attempt to shed further light on the changes throughout the time-series a PCA has been created in figure 8.23. It's made out of normalized values for each compound-like group, paired with each samples average peak area and armaticity index. The PCA was further run trough a k-clustering, which is added to the plot as colour.

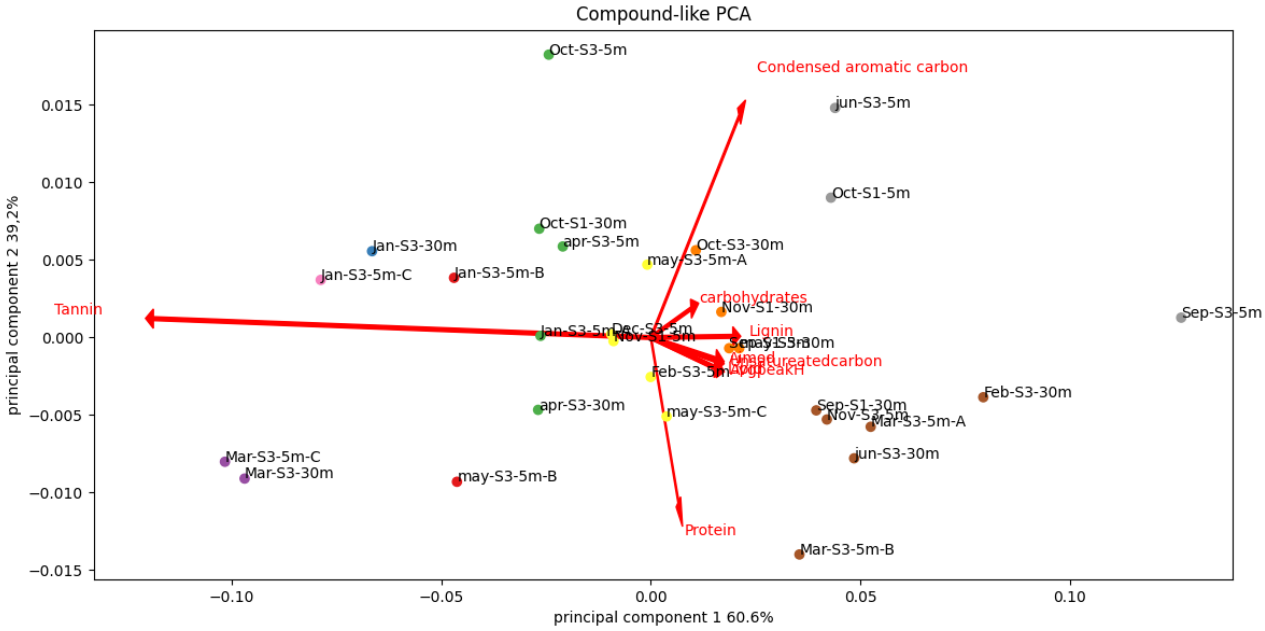

Figure 8.23: PCA of the normalized change in the compound-like distribution, paired with the change in average peak area and change in the Aromaticity index. Colour in with clusters based on k-mean clustering.

9 Discussion

This thesis set out to look at the seasonal changes of the molecular composition of DOM in a fjord environment.

The springtime data showed a clear increase of DOC. as well as chemical differentiation from the rest of the time series. The analysis suggest that springtime samples uniqueness comes primarily from the lignin and protein-like fractions of the compound-like groups. In addition to this there's a significant event happening in and around October, signified by increased DOC and chemical differentiation based on the condensed aromatic carbon-like fraction.

The DOC results in figure 8.1 indicate 2 separate instances of arctic DOM production or influx. This is happening in spring and late autumn. For the spring samples the the DOC peak is 1 month later for 30m as opposed to the 5m, which could signify a lag of bloom at the lower depth. Henson et al[66] show that such an affect happens and is related to the reach of solar radiation in the water column, which increased over springtime. In addition to this the 30m samples of the outer station show a larger and shorter peak, this peak could in this context be relate to a more explosive bloom as the depth increases. Although as there is an increased amount of variance at the time, show in figure 8.4 and figure 8.5 and time between sampling is one month while the bloom can last for a short amount of time. As such an analysis, with a higher frequency of sampling would be needed. moreover the longer height in 5m samples of figure 8.4, would indicate that there is another effect then the bloom maintaining the large concentration of DOC. In late autumn the increase, shown in 8.1, happens simultaneously as the death of phytoplancton in late autumn, from Yasemin B et al. in prep[67]. This could be an indicator of DOM coming from an autumn bloom. Although the fact that the increase happens almost exclusively to the 30m depth samples, is a again a contradicting factor to the current understanding of the bloom. as the higher death samples would be expected to have this bloom as well, at account of the larger amount of solar radiation. So if there's some factor limiting this the bloom or consuming the DOC created. Furthermore the inner sample having their DOC increase prior to the outer samples would indicate that there that there's a lag between locations, which could be cause by different photic zone as proposed by (Goebel et al[68]

Continuing to the SPE results, the PCoA in figure 8.14 Distinctly show that PCoA1 contains the most deviation and as such the springtime is the most active, with the May and March samples having the most significant deviation from the rest. This clear differentiation from the DOC result, figure 8.1. This could be cause by consummation being a more influential cause of chemical alteration.[] November point in PCoA figure 8.14 has the same differentiation as the march and may samples with the October, but instead of a month difference the difference is in the depths. With the high DOC samples of figure 8.1 staying within the biggest cluster and the samples with relatively stable DOC containing the differentiation, that being the 5m depth samples. This happens at the time of decline of picophytoplankton for Yasemin B et al. in prep[67]. Over all it's predominance of statistical differentiation in the 5m samples of the PCoAs, figures 8.8, 8.10, 8.12 and 8.14. Is to be expected as there is a increase of chemical influx, sunlight and organic activity. Xu et al[69] claimed that DOM with higher O/C is not easily degraded, and as such would explain the reason for the limitation number high Pearsons coeffitient R values for compounds with the higher O/C. Shown in the Van Krevelen plots at of figures 8.8, 8.10, 8.12 and 8.14. When looking only at the 5m samples in the PCoA of figure 8.10. There's significantly more homologous despite the previously claimed conjecture that there's more activity. This is likely simply the fact that the activity level remains more active over a longer period and therefor the points of activity don't cause as great of a differentiation between samples.

Moving on to the compound-like distribution the dominance of lignin is to expected from an environment where heavily impacted by the influx of terrestrial water. The low variance indicate that the primary reason for significantly higher amount of lignin comes from the fact that most of the lignin is not consumed. The Pearson plots showed a large number of significant peaks within the lignin-like fraction, showing the fact that despite low variation for the lignin-like fraction as a whole, there is still large amount of activity happening in this fraction that's not picked out by this method. Tannin-like follows as the second largest seconds the theory that input causing the largest amount of compounds in the column is the terrestrial.

The March samples show in figure 8.23 in the protein and tannin -like part of the PCA, the differentiation being much like that of the dendrogram and PCoAs in figures 8.15 and 8.14 respectively. Protein is significant as it indicates

phytoplankton as a important source, while lignin is primary terrestrial, so it would be assumed that that these happens because of a combination of terrestrial influx and phytoplankton bloom. The May samples less so affected by tannin, is possibly even more related to the bloom event. Based on this it's likely that the process causing these fractions growth are not the same process as the ones increasing the total DOC. These sample also showed up as the samples least like the rest in the dendrograms 8.15, 8.9, 8.11 and 8.13. Although in this plot the July samples were also in that group. Indicating the hierarchical clustering method picked up a variation not shown in the compound distribution method. Further figure 8.23 show that there is a negative correlation between the lignin and tannin -like compounds, which goes against the current understanding as it would be expected that these compounds would have similar sources and with there being low amount of research done, in the field of DOM, on oceanic tannin. There being sources and/or sinks large enough to create a negative correlation between these compound-like groups is yet to be introduced.

With the sampling starting in September and ending in august there not necessarily a correlation between the samples presented as 1 month away from each other as they are 1 year apart. The presentation of data as if going from January to December was done for the sake of simplicity. That being said the comparison done between sample as if they were one month away from each other are still relevant even if they are weakened. The peak in figure 8.3 is somewhat weakened as to if it's a peak.

Since there has been found evidence of SPE being better at containing lignin and tannin within the solid phase then that of protein and as such are over represent in the data. The over all ratio of these compound compared to the rest is in such a magnitude that the ratio of lignin and tannin to the rest is still big. there doesn't seam to be any big differences for these compound groups. When look at the differences for the inner and outer sample or for the 5m or 30m depths. This especially reduces the accuracy of the other compound like groups like protein and condensed aromatic structures. But also opens up the possibility of increased activity groups. This also be argued for in the recoveries data from figure 8.7 and table 8.3 as the recoveries samples of sample dates, in which the SPE samples from PCA 8.23 showed more effected by protein and condensed aromatic carbon -like compounds as opposed to lignin and tannin -like compounds, there's higher recovery. Although the loss over recovery is to such a large extent that it's likely

that the formic acid theorised to from a incomplete purge of the cartridge is a significant part of the low recovery.

10 Conclusion

The overall result of the time series, would indicate at least three separate points of major change if molecular DOM composition in Ramfjorden. Those happening twice in spring and once in autumn the year of sampling. Which composition influxes indicative of the spring and autumn bloom, as well as influx other compounds indicating the importance of other factors such as melt water. Further more there is a indication that the biggest chemical change in DOM is not directly from the increase of DOM in the water column, but rather the chemical changes happening prior to the major increase. Moreover there is a negative correlation between tannin and lignin -like compounds. For future there is a need to understand how DOM differ throughout the spring autumn, especially the identification of the cause of the divide between the two identified instances in spring. As well as an explanation for the negative correlation between tannin and lignin -like compounds.

References

[1] D. A. Hansell, C. A. Carlson, D. J. Repeta, and R. Schlitzer, "Dissolved organic matter in the ocean: A controversy stimulates new insights," *Oceanography (Washington, D.C.)*, vol. 22, no. 4, pp. 202–211, 2009.

[2] R. Benner, B. Von Bodungen, J. Farrington, J. Hedges, C. Lee, F. Mantoura, Y. Suzuki, and P. Williams, "Measurement of dissolved organic carbon and nitrogen in natural waters: Workshop report," *Marine chemistry*, vol. 41, no. 1, pp. 5–10, 1993.

[3] J. C. G. Walker, P. B. Hays, and J. F. Kasting, "A negative feedback mechanism for the long-term stabilization of earth's surface temperature," *Journal of Geophysical Research*, vol. 86, no. C10, pp. 9776–9782, 1981.

[4] E. B. Kujawinski, "The impact of microbial metabolism on marine dissolved organic matter," *Annual Review of Marine Science*, vol. 3, no. 1, pp. 567–599, 2011. PMID: 21329217.

[5] E. B. Kujawinski, "The impact of microbial metabolism on marine dissolved organic matter," *Annual review of marine science*, vol. 3, pp. 567–599, 2011.

[6] T. Dittmar, B. Koch, N. Hertkorn, and G. Kattner, "A simple and efficient method for the solid-phase extraction of dissolved organic matter (spe-dom) from seawater: Spe-dom from seawater," *Limnology and oceanography, methods*, vol. 6, no. 6, pp. 230–235, 2008.

[7] G. M. Perillo, "Chapter 2 definitions and geomorphologic classifications of estuaries," in *Geomorphology and Sedimentology of Estuaries* (G. Perillo, ed.), vol. 53 of *Developments in Sedimentology*, pp. 17–47, Elsevier, 1995.

[8] D. M. Farmer and H. J. Freeland, "The physical oceanography of fjords," *Progress in Oceanography*, vol. 12, no. 2, pp. 147–219, 1983.

[9] N. J. Fraser, R. Skogseth, F. Nilsen, and M. E. Inall, "Circulation and exchange in a broad arctic fjord using glider-based observations," *Polar research*, vol. 37, no. 1, pp. 1485417–19, 2018.

[10] K. R. Arrigo, D. K. Perovich, R. S. Pickart, Z. W. Brown, G. L. van Dijken, K. E. Lowry, M. M. Mills, M. A. Palmer, W. M. Balch, N. R. Bates, C. R. Benitez-Nelson, E. Brownlee, K. E. Frey, S. R. Laney, J. Mathis,

A. Matsuoka, B. Greg Mitchell, G. Moore, R. A. Reynolds, H. M. Sosik, and J. H. Swift, "Phytoplankton blooms beneath the sea ice in the chukchi sea," *Deep-sea research. Part II, Topical studies in oceanography*, vol. 105, pp. 1–16, 2014.

[11] D. V. Hansen and M. Rattray, "New dimensions in estuary classification," *Limnology and oceanography*, vol. 11, no. 3, pp. 319–326, 1966.

[12] "Biogeochemistry of marine dissolved organic matter," 2015.

[13] T. Volk and M. I. Hoffert, "Ocean carbon pumps: Analysis of relative strengths and efficiencies in ocean-driven atmospheric co2 changes," *The carbon cycle and atmospheric CO2: natural variations Archean to present*, vol. 32, pp. 99–110, 1985.

[14] B. Hönisch, A. Ridgwell, D. Schmidt, E. Thomas, S. Gibbs, A. Sluijs, R. Zeebe, L. Kump, R. Martindale, S. Greene, W. Kiessling, J. Ries, J. Zachos, D. Royer, S. Barker, T. Marchitto Jr., R. Moyer, C. Pelejero, P. Ziveri, G. Foster, and B. Williams, "The geological record of ocean acidification," *Science (American Association for the Advancement of Science)*, vol. 335, no. 6072, pp. 1058–1063, 2012.

[15] C. R. McClain, G. C. Feldman, D. A. Siegel, J. L. Sarmiento, A. J. Milligan, R. T. O'Malley, P. G. Falkowski, R. M. Letelier, E. S. Boss, and M. J. Behrenfeld, "Climate-driven trends in contemporary ocean productivity," *Nature*, vol. 444, no. 7120, pp. 752–755, 2006.

[16] A. Calbet and M. R. Landry, "Phytoplankton growth, microzooplankton grazing, and carbon cycling in marine systems," *Limnology and oceanography*, vol. 49, no. 1, pp. 51–57, 2004.

[17] U. Sommer, Z. M. Gliwicz, W. Lampert, and A. Duncan, "The peg-model of seasonal succession of planktonic events in fresh waters," *Archiv für Hydrobiologie*, vol. 106, no. 4, pp. 433–471, 1986.

[18] J. S. Fritz, "Solid-phase extraction: principles, techniques and applications edited by nigel j. k. simpson (varian associates). dekker: new york and basel. 2000. xi + 514 pp. 195.00. isbn 0-8247-09021-x," *Journal of the American Chemical Society*, vol. 122, no. 49, pp. 12411–12412, 2000.

[19] T. Dittmar, B. Koch, N. Hertkorn, and G. Kattner, "A simple and efficient

method for the solid-phase extraction of dissolved organic matter (spe-dom) from seawater," *Limnology and oceanography, methods*, vol. 6, no. 6, pp. 230–235, 2008.

[20] M. Chen, S. Kim, J.-E. Park, H. S. Kim, and J. Hur, "Effects of dissolved organic matter (dom) sources and nature of solid extraction sorbent on recoverable dom composition: Implication into potential lability of different compound groups," *Analytical and bioanalytical chemistry*, vol. 408, no. 17, pp. 4809–4819, 2016.

[21] L. Li, Z. Fang, C. He, and Q. Shi, "Separation and characterization of marine dissolved organic matter (dom) by combination of fe(oh)3 co-precipitation and solid phase extraction followed by esi ft-icr ms," *Analytical and bioanalytical chemistry*, vol. 411, no. 10, pp. 2201–2208, 2019.

[22] S. Kim, D. Kim, M. Jung, and S. Kim, "Analysis of environmental organic matters by ultrahigh-resolution mass spectrometry—a review on the development of analytical methods," *Mass spectrometry reviews*, vol. 41, no. 2, pp. 352–369, 2022.

[23] A. Linkhorst, T. Dittmar, and H. Waska, "Molecular fractionation of dissolved organic matter in a shallow subterranean estuary: The role of the iron curtain," *Environmental Science and Technology*, vol. 51, no. 3, pp. 1312–1320, 2017.

[24] M. P. Bhatia, S. B. Das, K. Longnecker, M. A. Charette, and E. B. Kujawinski, "Molecular characterization of dissolved organic matter associated with the greenland ice sheet," *Geochimica et cosmochimica acta*, vol. 74, no. 13, pp. 3768–3784, 2010.

[25] Y. Sugimura and Y. Suzuki, "A high-temperature catalytic oxidation method for the determination of non-volatile dissolved organic carbon in seawater by direct injection of a liquid sample," *Marine chemistry*, vol. 24, no. 2, pp. 105–131, 1988.

[26] R. H. Perry, R. G. Cooks, and R. J. Noll, "Orbitrap mass spectrometry: Instrumentation, ion motion and applications," *Mass spectrometry reviews*, vol. 27, no. 6, pp. 661–699, 2008.

[27] O. Lange, E. Damoc, A. Wieghaus, and A. Makarov, "Enhanced fourier

transform for orbitrap mass spectrometry," *International Journal of Mass Spectrometry*, vol. 369, pp. 16–22, 2014.

[28] C. Benecke, R. Grund, R. Hohberger, A. Kerber, R. Laue, and T. Wieland, "Molgen +, a generator of connectivity isomers and stereoisomers for molecular structure elucidation," *Analytica chimica acta*, vol. 314, no. 3, pp. 141–147, 1995.

[29] B. P. Koch and T. Dittmar, "From mass to structure: an aromaticity index for high-resolution mass data of natural organic matter," *Rapid communications in mass spectrometry*, vol. 30, no. 1, pp. 250–250, 2016.

[30] D. W. Van Krevelen, "Graphical-statistical method for the study of structure and reaction process of coal," vol. 29, p. 269284, 1950.

[31] V. Mangal, N. L. Stock, and C. Guéguen, "Molecular characterization of phytoplankton dissolved organic matter (dom) and sulfur components using high resolution orbitrap mass spectrometry," *Analytical and bioanalytical chemistry*, vol. 408, no. 7, pp. 1891–1900, 2016.

[32] W. Xu, Q. Gao, C. He, Q. Shi, Z.-Q. Hou, and H.-Z. Zhao, "Using esi ft-icr ms to characterize dissolved organic matter in salt lakes with different salinity," *Environmental science technology*, vol. 54, no. 20, pp. 12929–12937, 2020.

[33] J. R. Laszakovits and A. A. MacKay, "Data-based chemical class regions for van krevelen diagrams," *Journal of the American Society for Mass Spectrometry*, vol. 33, no. 1, pp. 198–202, 2022.

[34] G. de Gonzalo, D. I. Colpa, M. H. Habib, and M. W. Fraaije, "Bacterial enzymes involved in lignin degradation," *Journal of biotechnology*, vol. 236, pp. 110–119, 2016.

[35] K. Sarkanen and C. Schuerch, "Conductometric determination of phenolic groups in mixtures such as isolated lignins," *Analytical Chemistry*, vol. 27, no. 8, pp. 1245–1250, 1955.

[36] W. C. Hockaday, J. M. Purcell, A. G. Marshall, J. A. Baldock, and P. G. Hatcher, "Electrospray and photoionization mass spectrometry for the characterization of organic matter in natural waters: a qualitative assessment," *Limnology and oceanography, methods*, vol. 7, no. 1, pp. 81–95, 2009.

[37] R. Mutabaruka, K. Hairiah, and G. Cadisch, "Microbial degradation of hydrolysable and condensed tannin polyphenol–protein complexes in soils from different land-use histories," *Soil biology biochemistry*, vol. 39, no. 7, pp. 1479–1492, 2007.

[38] W. Bowden, T. Riis, and J. Glime, "Macrophytes and bryophytes," 2017.

[39] S. Liu, Z. He, Z. Tang, L. Liu, J. Hou, T. Li, Y. Zhang, Q. Shi, J. P. Giesy, and F. Wu, "Linking the molecular composition of autochthonous dissolved organic matter to source identification for freshwater lake ecosystems by combination of optical spectroscopy and ft-icr-ms analysis," *The Science of the total environment*, vol. 703, pp. 134764–134764, 2020.

[40] N. Ridgway, R. McLeod, and D. E. Vance, *Biochemistry of Lipids, Lipoproteins and Membranes*. Amsterdam: Elsevier Science Technology, 2008.

[41] S. Liu, Z. He, Z. Tang, L. Liu, J. Hou, T. Li, Y. Zhang, Q. Shi, J. P. Giesy, and F. Wu, "Linking the molecular composition of autochthonous dissolved organic matter to source identification for freshwater lake ecosystems by combination of optical spectroscopy and ft-icr-ms analysis," *The Science of the total environment*, vol. 703, pp. 134764–134764, 2020.

[42] A. E. Hagerman and L. G. Butler, "Choosing appropriate methods and standards for assaying tannin," *Journal of Chemical Ecology*, vol. 15, no. 6, pp. 1795–1810, 1989.

[43] W. D. P. Stewart, *Algal physiology and biochemistry*, vol. 10. Univ of California Press, 1974.

[44] K. K. L. B. Adikaram, M. A. Hussein, M. Effenberger, and T. Becker, "Data transformation technique to improve the outlier detection power of grubbs' test for data expected to follow linear relation," *Journal of applied mathematics*, vol. 2015, pp. 1–9, 2015.

[45] S. J. Meyer, K. G. Hubbard, and D. A. Wilhite, "The relationship of climatic indices and variables to corn (maize) yields: a principal components analysis," *Agricultural and forest meteorology*, vol. 55, no. 1, pp. 59–84, 1991.

[46] N. Salem and S. Hussein, "Data dimensional reduction and principal components analysis," *Procedia Computer Science*, vol. 163, pp. 292–299, 2019.

[47] H. Abdi and L. J. Williams, "Principal component analysis," *Wiley interdisciplinary reviews. Computational statistics*, vol. 2, no. 4, pp. 433–459, 2010.

[48] W. A. Jensen and M. Alexander, "Statistics for engineering and the sciences, 6th edition," *Journal of Quality Technology*, vol. 48, no. 3, pp. 297–299, 2016.

[49] H. BOCK, "Algorithms for clustering data - jain,ak, dubes,rc," vol. 6, no. 1, pp. 126–128, 1989.

[50] M. Forina, C. Armanino, and V. Raggio, "Clustering with dendrograms on interpretation variables," *Analytica chimica acta*, vol. 454, no. 1, pp. 13–19, 2002.

[51] J. Andrade and M. Estévez-Pérez, "Statistical comparison of the slopes of two regression lines: A tutorial," *Analytica chimica acta*, vol. 838, pp. 1–12, 2014.

[52] Kiatdd. https://commons.wikimedia.org/w/index.php?curid=37108966, 2012.

[53] N. Balakrishnan, V. Voinov, and M. Nikulin, "Chapter 2 - pearson's sum and pearson-fisher test," in *Chi-Squared Goodness of Fit Tests with Applications*, pp. 11–26, Elsevier Inc, 2013.

[54] J. Benesty, J. Chen, Y. Huang, and I. Cohen, "Pearson correlation coefficient," in *Noise reduction in speech processing*, pp. 1–4, Springer, 2009.

[55] T. F. Cox, "Multidimensional scaling," 2001.

[56] I. Borg, "Modern multidimensional scaling : theory and applications," 1997.

[57] M. O'Sadnick, C. Petrich, C. Brekke, and J. Skarðhamar, "Ice extent in sub-arctic fjords and coastal areas from 2001 to 2019 analyzed from modis imagery," *Annals of glaciology*, vol. 61, no. 82, pp. 210–226, 2020.

[58] 2022.

[59] M. G. Digernes, "personal communication," 2022.

[60] MATLAB, *version 7.10.0 (R2010a)*. Natick, Massachusetts: The MathWorks Inc., 2010.

[61] A. Nebbioso and A. Piccolo, "Molecular characterization of dissolved organic matter (dom): a critical review," *Analytical and bioanalytical chemistry*, vol. 405, no. 1, pp. 109–124, 2012.

[62] J. D. Hunter, "Matplotlib: A 2d graphics environment," *Computing in Science & Engineering*, vol. 9, no. 3, pp. 90–95, 2007.

[63] F. Pedregosa, G. Varoquaux, A. Gramfort, V. Michel, B. Thirion, O. Grisel, M. Blondel, P. Prettenhofer, R. Weiss, V. Dubourg, J. Vanderplas, A. Passos, D. Cournapeau, M. Brucher, M. Perrot, and E. Duchesnay, "Scikit-learn: Machine learning in Python," *Journal of Machine Learning Research*, vol. 12, pp. 2825–2830, 2011.

[64] T. pandas development team, "pandas-dev/pandas: Pandas," Feb. 2020.

[65] C. R. Harris, K. J. Millman, S. J. van der Walt, R. Gommers, P. Virtanen, D. Cournapeau, E. Wieser, J. Taylor, S. Berg, N. J. Smith, R. Kern, M. Picus, S. Hoyer, M. H. van Kerkwijk, M. Brett, A. Haldane, J. F. del Río, M. Wiebe, P. Peterson, P. Gérard-Marchant, K. Sheppard, T. Reddy, W. Weckesser, H. Abbasi, C. Gohlke, and T. E. Oliphant, "Array programming with NumPy," *Nature*, vol. 585, pp. 357–362, Sept. 2020.

[66] S. A. Henson, I. Robinson, J. T. Allen, and J. J. Waniek, "Effect of meteorological conditions on interannual variability in timing and magnitude of the spring bloom in the irminger basin, north atlantic," *Deep-sea research. Part I, Oceanographic research papers*, vol. 53, no. 10, pp. 1601–1615, 2006.

[67] M. A.-A. S. G. K. M. L. P. Yasemin Bodur, Maria Guadalupe Digernes, "Seasonal aggregation potential of dissolved organic matter (dom) in an arctic fjord," et al. in prep.

[68] N. Goebel, S. Wing, and P. Boyd, "A mechanism for onset of diatom blooms in a fjord with persistent salinity stratification," *Estuarine, coastal and shelf science*, vol. 64, no. 2, pp. 546–560, 2005.

[69] W. Xu, Q. Gao, C. He, Q. Shi, Z.-Q. Hou, and H.-Z. Zhao, "Using esi ft-icr ms to characterize dissolved organic matter in salt lakes with different salinity," *Environmental science technology*, vol. 54, no. 20, pp. 12929–12937, 2020.

11 Appendix a

Month	Sample Name	Concentration	Area	Date / Time
January	Jan St3 5m 1	0.81860	9.067	2/5/2022 11:22:33 PM
	Jan St3 5m 1	0.85240	9.357	2/5/2022 11:25:12 PM
	Jan St3 5m 1	0.90550	9.813	2/5/2022 11:27:55 PM
	Jan St3 5m 2	1.10300	11.51	2/5/2022 11:34:19 PM
	Jan St3 5m 2	1.00800	10.69	2/5/2022 11:37:12 PM
	Jan St3 5m 2	1.05700	11.11	2/5/2022 11:40:17 PM
	Jan St3 5m 3	1.54700	15.32	2/5/2022 11:57:37 PM
	Jan St3 5m 3	1.50900	14.99	2/6/2022 12:00:22 AM
	Jan St3 30m 1	1.29400	13.15	2/5/2022 9:53:50 PM
	Jan St3 30m 1	1.20100	12.35	2/5/2022 9:56:41 PM
	Jan St3 30m 1	1.22400	12.55	2/5/2022 9:59:29 PM
	Jan St3 30m 2	0.82280	9.103	2/5/2022 10:04:46 PM
	Jan St3 30m 2	0.81420	9.029	2/5/2022 10:07:27 PM
	Jan St3 30m 3	0.98440	10.49	2/5/2022 10:16:05 PM
	Jan St3 30m 3	0.96230	10.30	2/5/2022 10:18:48 PM
	Jan blank 1	0.00275	2.064	2/6/2022 12:38:00 AM
	Jan blank 1	0.05646	2.525	2/6/2022 12:40:15 AM
	Jan blank 1	0.03945	2.379	2/6/2022 12:42:26 AM
	Jan blank 2	0.88930	9.674	2/6/2022 12:15:55 AM
	Jan blank 2	0.95760	10.26	2/6/2022 12:18:11 AM
	Jan blank 2	0.95880	10.27	2/6/2022 12:20:28 AM
	Jan blank 3	0.22110	3.938	2/6/2022 12:27:06 AM
	Jan blank 3	0.27020	4.360	2/6/2022 12:29:21 AM
	Jan blank 3	0.27820	4.428	2/6/2022 12:31:44 AM
February	Feb st3 5m 1	1.39500	14.01	2/9/2022 1:00:42 AM
	Feb st3 5m 1	1.39000	13.97	2/9/2022 1:03:18 AM
	Feb st3 5m 2	1.61500	15.90	2/9/2022 1:12:10 AM
	Feb st3 5m 2	1.57200	15.53	2/9/2022 1:15:17 AM
	Feb st3 5m 3	2.44000	22.98	2/9/2022 1:31:37 AM
	Feb st3 5m 3	2.46300	23.18	2/9/2022 1:34:30 AM
	Feb st3 30m 1	0.97390	10.40	2/8/2022 11:20:43 PM
	Feb st3 30m 1	0.96580	10.33	2/8/2022 11:23:27 PM
	Feb st3 30m 2	3.62400	33.15	2/8/2022 11:31:58 PM

	Feb st3 30m 2	3.56100	32.61	2/8/2022 11:34:40 PM
	Feb st3 30m 3	1.32100	13.38	2/8/2022 11:43:32 PM
	Feb st3 30m 3	1.28700	13.09	2/8/2022 11:46:21 PM
March	Mar st3 5m 1	3.35600	31.01	2/15/2022 9:26:22 PM
	Mar st3 5m 1	3.28500	30.39	2/15/2022 9:29:15 PM
	Mar st3 5m 2	1.15700	11.94	2/15/2022 10:23:30 PM
	Mar st3 5m 2	1.11500	11.57	2/15/2022 10:26:06 PM
	Mar st3 5m 2	1.09900	11.43	2/15/2022 10:28:57 PM
	Mar st3 5m 3	1.16300	11.99	2/15/2022 10:34:19 PM
	Mar st3 5m 3	1.16000	11.96	2/15/2022 10:36:55 PM
	Mar St 3 30m 1	1.25500	12.79	2/15/2022 8:52:24 PM
	Mar St 3 30m 1	1.24000	12.66	2/15/2022 8:54:58 PM
	Mar St 3 30m 2	1.32800	13.42	2/15/2022 9:03:35 PM
	Mar St 3 30m 2	1.29500	13.13	2/15/2022 9:06:12 PM
	Mar St 3 30m 3	2.68600	25.20	2/15/2022 9:14:40 PM
	Mar St 3 30m 3	2.65200	24.90	2/15/2022 9:17:18 PM
	Mar blank 1	0.39240	5.307	2/15/2022 10:45:18 PM
	Mar blank 1	0.41630	5.514	2/15/2022 10:47:52 PM
	Mar blank 1	0.36320	5.054	2/15/2022 10:50:10 PM
	Mar blank 2	0.25990	4.158	2/15/2022 10:56:09 PM
	Mar blank 2	0.25890	4.149	2/15/2022 10:58:26 PM
	Mar blank 3	1.12300	11.64	2/15/2022 11:07:24 PM
	Mar blank 3	1.08200	11.29	2/15/2022 11:09:43 PM
	Mar blank 3	1.12500	11.66	2/15/2022 11:12:09 PM
April	Apr st3 5m 1	7.20700	64.40	2/15/2022 6:53:33 PM
	Apr st3 5m 1	6.97400	62.38	2/15/2022 6:56:26 PM
	Apr st3 5m 1	6.94400	62.12	2/15/2022 6:59:25 PM
	Apr st3 5m 2	3.38800	31.28	2/15/2022 7:04:49 PM
	Apr st3 5m 2	3.30200	30.54	2/15/2022 7:07:41 PM
	Apr st3 5m 3	2.04200	19.61	2/15/2022 7:59:27 PM
	Apr st3 5m 3	1.98200	19.09	2/15/2022 8:02:10 PM
	Apr st3 30m 1	5.39000	48.64	2/15/2022 8:11:00 PM
	Apr st3 30m 1	5.23800	47.33	2/15/2022 8:14:04 PM
	Apr st3 30m 2	8.25100	73.45	2/15/2022 8:30:53 PM
	Apr st3 30m 2	8.17600	72.80	2/15/2022 8:34:04 PM
	Apr st3 30m 3	7.08100	63.31	2/15/2022 8:41:58 PM

	Apr st3 30m 3	6.95100	62.18	2/15/2022 8:44:58 PM
May	May st3 5m 1	19.87000	174.2	2/15/2022 7:14:49 AM
	May st3 5m 1	19.57000	171.6	2/15/2022 7:18:25 AM
	May st3 5m 2	1.60200	15.80	2/15/2022 7:34:44 AM
	May st3 5m 2	1.60000	15.78	2/15/2022 7:37:29 AM
	May st3 5m 3	74.78000	650.4	2/15/2022 7:47:29 AM
	May st3 5m 3	73.13000	636.1	2/15/2022 7:51:07 AM
	May st3 30m 1	3.97300	36.36	2/15/2022 7:57:06 AM
	May st3 30m 1	3.90000	35.72	2/15/2022 8:00:00 AM
	May st3 30m 2	3.34000	30.87	2/15/2022 8:08:24 AM
	May st3 30m 2	3.32000	30.69	2/15/2022 8:11:21 AM
	May st3 30m 3	2.64300	24.82	2/15/2022 1:18:48 PM
	May st3 30m 3	2.66700	25.03	2/15/2022 1:21:35 PM
	May Blank 1	4.18700	38.21	2/15/2022 1:30:22 PM
	May Blank 1	4.09000	37.37	2/15/2022 1:33:18 PM
	May Blank 2	6.09500	54.76	2/15/2022 1:52:28 PM
	May Blank 2	5.99400	53.88	2/15/2022 1:55:28 PM
	May Blank 3	5.52000	49.77	2/15/2022 2:14:07 PM
	May Blank 3	5.46200	49.27	2/15/2022 2:17:05 PM
June	June st3 5m 1	2.31400	21.97	2/15/2022 12:44:51 AM
	June st3 5m 1	2.28400	21.71	2/15/2022 12:47:32 AM
	June st3 5m 2	2.57300	24.22	2/15/2022 12:56:13 AM
	June st3 5m 2	2.52400	23.79	2/15/2022 12:59:03 AM
	June st3 5m 2	2.11600	20.25	2/15/2022 1:56:09 AM
	June st3 5m 3	2.04600	19.65	2/15/2022 1:58:55 AM
	June st3 5m 3	2.06000	19.77	2/15/2022 2:01:42 AM
	June st3 30m 1	1.25200	12.76	2/15/2022 2:07:03 AM
	June st3 30m 1	1.23100	12.58	2/15/2022 2:09:41 AM
	June st3 30m 2	6.62300	59.34	2/15/2022 2:19:01 AM
	June st3 30m 2	6.56300	58.82	2/15/2022 2:22:06 AM
	June st3 30m 3	2.20200	21.00	2/15/2022 2:29:19 AM
	June st3 30m 3	2.17000	20.72	2/15/2022 2:31:55 AM
July	July st1 5m 1	181.20000	1573	2/14/2022 9:45:27 PM
	July st1 5m 1	181.60000	1577	2/14/2022 9:49:39 PM
	July st1 5m 2	58.81000	511.9	2/14/2022 9:55:38 PM
	July st1 5m 2	58.52000	509.4	2/14/2022 9:58:59 PM

	July st1 5m 3	74.83000	650.8	2/14/2022 10:07:02 PM
	July st1 5m 3	73.57000	639.9	2/14/2022 10:10:35 PM
	July st1 30m 1	1.64600	16.18	2/14/2022 10:16:43 PM
	July st1 30m 1	1.65300	16.24	2/14/2022 10:19:25 PM
	July st1 30m 2	1.23600	12.62	2/14/2022 10:27:46 PM
	July st1 30m 2	1.23200	12.59	2/14/2022 10:30:27 PM
	July st1 30m 3	50.56000	440.3	2/14/2022 10:40:32 PM
	July st1 30m 3	50.27000	437.8	2/14/2022 10:44:09 PM
	July st3 5m 1	1.75200	17.10	2/14/2022 7:40:51 PM
	July st3 5m 1	1.51100	15.01	2/14/2022 7:43:31 PM
	July st3 5m 1	1.47400	14.69	2/14/2022 7:46:07 PM
	July st3 5m 2	1.63200	16.06	2/14/2022 7:51:27 PM
	July st3 5m 2	1.62800	16.02	2/14/2022 7:54:13 PM
	July st3 5m 3	63.98000	556.7	2/14/2022 8:04:03 PM
	July st3 5m 3	62.98000	548.0	2/14/2022 8:07:42 PM
	July st3 30m 1	1.70700	16.71	2/14/2022 8:13:43 PM
	July st3 30m 1	1.70500	16.69	2/14/2022 8:16:39 PM
	July Blank 1	0.85770	9.342	2/14/2022 11:38:07 PM
	July Blank 1	0.86940	9.443	2/14/2022 11:40:36 PM
	July Blank 2	118.90000	1033	2/15/2022 12:02:06 AM
	July Blank 2	120.40000	1046	2/15/2022 12:06:32 AM
	July Blank 3	0.15010	3.206	2/15/2022 12:22:09 AM
	July Blank 3	0.13540	3.078	2/15/2022 12:24:18 AM
August	Aug st3 5m 1	1.56600	16.18	3/2/2022 6:49:52 PM
	Aug st3 5m 1	1.53300	15.90	3/2/2022 6:52:33 PM
	Aug st3 5m 2	2.43500	23.02	2/14/2022 2:15:53 PM
	Aug st3 5m 2	2.41700	22.86	2/14/2022 2:18:52 PM
	Aug st3 5m 3	3.17300	29.42	2/14/2022 2:27:08 PM
	Aug st3 5m 3	3.16000	29.31	2/14/2022 2:30:00 PM
	Aug st3 30m 1	1.53100	15.18	2/14/2022 2:37:59 PM
	Aug st3 30m 1	1.47100	14.66	2/14/2022 2:40:34 PM
	Aug st3 30m 1	1.49100	14.83	2/14/2022 2:43:16 PM
	Aug st3 30m 2	1.12700	11.68	2/14/2022 2:49:03 PM
	Aug st3 30m 2	1.09500	11.40	2/14/2022 2:51:53 PM
	Aug st3 30m 3	1.44400	14.43	2/14/2022 3:00:02 PM
	Aug st3 30m 3	1.41400	14.17	2/14/2022 3:02:47 PM

September	Sep st1 5m 1	2.66800	24.94	2/9/2022 1:42:46 AM
	Sep st1 5m 1	2.55400	23.96	2/9/2022 1:45:27 AM
	Sep st1 5m 1	2.56200	24.03	2/9/2022 1:48:10 AM
	Sep st1 5m 2	2.28800	21.68	2/9/2022 1:53:39 AM
	Sep st1 5m 2	2.27200	21.54	2/9/2022 1:56:18 AM
	Sep st1 5m 3	1.38400	13.92	2/9/2022 2:04:54 AM
	Sep st1 5m 3	1.37800	13.87	2/9/2022 2:07:42 AM
	Sep st1 30m 1	2.57600	24.15	2/9/2022 2:16:05 AM
	Sep st1 30m 1	2.56400	24.05	2/9/2022 2:19:01 AM
	Sep st1 30m 2	3.05600	28.27	2/9/2022 2:27:18 AM
	Sep st1 30m 2	3.08800	28.55	2/9/2022 2:30:16 AM
	Sep st1 30m 3	1.58100	15.61	2/9/2022 3:43:57 AM
	Sep st1 30m 3	1.58400	15.64	2/9/2022 3:46:41 AM
	Sep st3 5m 1	1.30500	13.24	2/9/2022 3:55:11 AM
	Sep st3 5m 1	1.26500	12.90	2/9/2022 3:57:50 AM
	Sep st3 5m 2	1.76400	17.18	2/9/2022 4:06:09 AM
	Sep st3 5m 2	1.70100	16.64	2/9/2022 4:08:46 AM
	Sep st3 5m 2	1.70400	16.67	2/9/2022 4:11:28 AM
	Sep st3 5m 3	1.56600	15.48	2/9/2022 4:17:05 AM
	Sep st3 5m 3	1.59100	15.70	2/9/2022 4:19:55 AM
October	Oct St1 5m 1	2.97100	27.54	2/4/2022 6:01:34 PM
	Oct St1 5m 1	2.97500	27.58	2/4/2022 6:04:24 PM
	Oct St1 5m 2	1.34200	13.56	2/4/2022 6:12:34 PM
	Oct St1 5m 2	1.32000	13.37	2/4/2022 6:15:17 PM
	Oct St1 5m 3	2.48100	23.34	2/4/2022 6:23:43 PM
	Oct St1 5m 3	2.43300	22.92	2/4/2022 6:26:29 PM
	Oct St1 30m 1	3.51600	32.22	2/4/2022 6:34:40 PM
	Oct St1 30m 1	3.52100	32.26	2/4/2022 6:37:38 PM
	Oct St1 30m 2	2.80500	26.12	2/4/2022 6:46:03 PM
	Oct St1 30m 2	2.74800	25.63	2/4/2022 6:48:51 PM
	Oct St1 30m 3	1.97500	18.99	2/4/2022 6:56:51 PM
	Oct St1 30m 3	1.90200	18.37	2/4/2022 6:59:27 PM
	Oct St1 30m 3	1.91300	18.46	2/4/2022 7:02:05 PM
	Oct St3 5m 1	1.83000	17.75	2/4/2022 7:07:43 PM
	Oct St3 5m 1	1.82900	17.74	2/4/2022 7:10:25 PM
	Oct St3 5m 2	1.19900	12.33	2/4/2022 7:19:19 PM

	Oct St3 5m 2	1.15200	11.93	2/4/2022 7:22:05 PM
	Oct St3 5m 2	1.15900	11.99	2/4/2022 7:24:56 PM
	Oct St3 5m 3	1.77200	17.25	2/4/2022 8:34:20 PM
	Oct St3 5m 3	1.77000	17.23	2/4/2022 8:37:01 PM
	Oct St3 30m 1	1.76000	17.15	2/4/2022 8:45:24 PM
	Oct St3 30m 1	1.75200	17.08	2/4/2022 8:48:13 PM
	Oct St3 30m 2	1.23800	12.67	2/4/2022 8:56:23 PM
	Oct St3 30m 2	1.24900	12.76	2/4/2022 8:59:10 PM
	Oct St3 30m 3	1.19800	12.32	2/4/2022 9:07:21 PM
	Oct St3 30m 3	1.15500	11.95	2/4/2022 9:10:04 PM
	Oct St3 30m 3	1.14300	11.85	2/4/2022 9:12:44 PM
November	Nov St1 5m 1	2.65300	24.81	2/5/2022 3:06:00 AM
	Nov St1 5m 1	2.61800	24.51	2/5/2022 3:08:41 AM
	Nov St1 5m 2	1.31200	13.30	2/5/2022 3:17:08 AM
	Nov St1 5m 2	1.27300	12.97	2/5/2022 3:19:47 AM
	Nov St1 5m 3	5.69000	50.88	2/5/2022 4:36:32 AM
	Nov St1 5m 3	5.69200	50.90	2/5/2022 4:39:35 AM
	Nov st1 30m 1	1.58900	16.37	3/2/2022 6:27:40 PM
	Nov st1 30m 1	1.49700	15.60	3/2/2022 6:30:10 PM
	Nov st1 30m 1	1.47900	15.45	3/2/2022 6:32:42 PM
	Nov st1 30m 2	2.49700	23.95	3/2/2022 6:38:35 PM
	Nov st1 30m 2	2.43200	23.41	3/2/2022 6:41:14 PM
	Nov St1 30m 3	0.91180	9.867	2/5/2022 3:54:08 PM
	Nov St1 30m 3	0.93780	10.09	2/5/2022 3:56:44 PM
	Nov St3 5m 1	46.39000	400.2	2/5/2022 4:48:36 AM
	Nov St3 5m 1	46.29000	399.4	2/5/2022 4:52:02 AM
	Nov St3 5m 2	38.98000	336.6	2/5/2022 4:59:29 AM
	Nov St3 5m 2	38.20000	329.9	2/5/2022 5:02:50 AM
	Nov St3 5m 3	1.04700	11.03	2/5/2022 5:09:39 AM
	Nov St3 5m 3	1.02900	10.87	2/5/2022 5:12:31 AM
	Nov St3 30m 1	1.63900	16.11	2/5/2022 5:20:36 AM
	Nov St3 30m 1	1.60300	15.80	2/5/2022 5:23:17 AM
	Nov St3 30m 2	2.59400	24.31	2/5/2022 5:32:08 AM
	Nov St3 30m 2	2.55800	24.00	2/5/2022 5:35:00 AM
December	Dec St3 5m 2	1.01200	10.73	2/5/2022 7:27:31 PM

Dec St3 5m 2	1.04800	11.04	2/5/2022 7:30:30 PM
Dec St3 5m 2	1.04800	11.04	2/5/2022 7:33:08 PM
Dec St3 5m 3	1.04400	11.00	2/5/2022 7:38:39 PM
Dec St3 5m 3	1.06700	11.20	2/5/2022 7:41:24 PM
Dec St3 30m 1	0.94600	10.16	2/5/2022 6:54:27 PM
Dec St3 30m 1	0.98090	10.46	2/5/2022 6:57:08 PM
Dec St3 30m 1	0.94250	10.13	2/5/2022 6:59:51 PM
Dec St3 30m 2	1.18200	12.19	2/5/2022 7:05:35 PM
Dec St3 30m 2	1.17400	12.12	2/5/2022 7:08:19 PM
Dec St3 30m 3	1.11000	11.57	2/5/2022 7:16:57 PM
Dec St3 30m 3	1.09200	11.41	2/5/2022 7:19:45 PM

[]

Sample Name	Concentration	Date run
Jan St3 5m 1	0.858833	2/5/2022 11:27:55 PM
Jan St3 5m 2	1.056000	2/5/2022 11:40:17 PM
Jan St3 5m 3	1.528000	2/6/2022 12:00:22 AM
Jan MQ blanc 2	0.935233	2/6/2022 12:20:28 AM
Jan MQ blanc 3	0.256500	2/6/2022 12:31:44 AM
Jan MQ blanc 1	0.032887	2/6/2022 12:42:26 AM
Jan St3 30m 1	1.239667	2/5/2022 9:59:29 PM
Jan St3 30m 2	0.818500	2/5/2022 10:07:27 PM
Jan St3 30m 3	0.973350	2/5/2022 10:18:48 PM
Mid QC	0.544267	2/6/2022 1:28:22 AM
MQ Blanc F	-0.176067	2/6/2022 1:48:10 AM
MQ Blanc A	-0.180900	2/6/2022 2:07:59 AM
Low QC	0.390833	2/6/2022 3:58:33 AM
QC Surface	0.762050	2/8/2022 4:26:11 PM
MQ blanc	-0.176950	2/8/2022 4:42:52 PM
MQ blanc	-0.181767	2/8/2022 5:02:02 PM
QC mid	0.646133	2/8/2022 6:59:53 PM
MQ Blanc	-0.191350	2/8/2022 7:16:29 PM
MQ Blanc	-0.176633	2/8/2022 7:35:34 PM
QC Deep	0.396000	2/8/2022 9:33:34 PM

MQ Blanc	-0.181000	2/8/2022 9:52:16 PM
MQ Blanc	-0.209500	2/8/2022 10:09:09 PM
Feb st3 30m 1	0.969850	2/8/2022 11:23:27 PM
Feb st3 30m 2	3.592500	2/8/2022 11:34:40 PM
Feb st3 30m 3	1.304000	2/8/2022 11:46:21 PM
QC Surface	0.754667	2/9/2022 12:08:22 AM
MQ Blanc	-0.178050	2/9/2022 12:24:58 AM
MQ Blanc	-0.178333	2/9/2022 12:44:35 AM
Feb st3 5m 1	1.392500	2/9/2022 1:03:18 AM
Feb st3 5m 2	1.593500	2/9/2022 1:15:17 AM
Feb st3 5m 3	2.451500	2/9/2022 1:34:30 AM
Mar St 3 30m 1	1.247500	2/15/2022 8:54:58 PM
Mar St 3 30m 2	1.311500	2/15/2022 9:06:12 PM
Mar St 3 30m 3	2.669000	2/15/2022 9:17:18 PM
Mar st3 5m 1	3.320500	2/15/2022 9:29:15 PM
QC mid	0.559100	2/15/2022 9:50:33 PM
MQ Blanc	-0.152150	2/15/2022 10:07:13 PM
Mar st3 5m 2	1.123667	2/15/2022 10:28:57 PM
Mar st3 5m 3	1.161500	2/15/2022 10:36:55 PM
Mar blanc 1	0.390633	2/15/2022 10:50:10 PM
Mar blanc 2	0.259400	2/15/2022 10:58:26 PM
Mar blanc 3	1.110000	2/15/2022 11:12:09 PM
QC Deep	0.371100	2/15/2022 11:24:18 PM
MQ Blanc	-0.133933	2/15/2022 11:43:11 PM
QC mid	0.617767	2/15/2022 3:01:14 PM
MQ Blanc	-0.119750	2/15/2022 3:18:05 PM
QC Deep	0.411050	2/15/2022 5:13:50 PM
MQ Blanc	-0.131350	2/15/2022 5:30:31 PM
Apr st3 5m 1	7.041667	2/15/2022 6:59:25 PM
Apr st3 5m 2	3.345000	2/15/2022 7:07:41 PM
QC surface	0.749050	2/15/2022 7:26:30 PM
MQ Blanc	-0.134950	2/15/2022 7:43:11 PM
Apr st3 5m 3	2.012000	2/15/2022 8:02:10 PM
Apr st3 30m 1	5.314000	2/15/2022 8:14:04 PM
Apr st3 30m 2	8.213500	2/15/2022 8:34:04 PM
Apr st3 30m 3	7.016000	2/15/2022 8:44:58 PM

May st3 5m 1	19.720000	2/15/2022 7:18:25 AM
May st3 5m 2	1.601000	2/15/2022 7:37:29 AM
May st3 5m 3	73.955000	2/15/2022 7:51:07 AM
May st3 30m 1	3.936500	2/15/2022 8:00:00 AM
May st3 30m 2	3.330000	2/15/2022 8:11:21 AM
QC Deep	0.427300	2/15/2022 8:24:14 AM
Instrument blanc	-0.126400	2/15/2022 8:40:50 AM
MQ Blanc	-0.127850	2/15/2022 11:51:37 AM
MQ Blanc	-0.129300	2/15/2022 12:10:32 PM
QC surface	0.807350	2/15/2022 12:45:57 PM
MQ Blanc	-0.145900	2/15/2022 1:02:37 PM
May st3 30m 3	2.655000	2/15/2022 1:21:35 PM
May Blanc 1A	4.138500	2/15/2022 1:33:18 PM
May Blanc 1B	1.112000	2/15/2022 1:45:12 PM
May Blanc 2A	6.044500	2/15/2022 1:55:28 PM
May Blanc 2B	0.452900	2/15/2022 2:04:30 PM
May Blanc 3A	5.491000	2/15/2022 2:17:05 PM
May Blanc 3B	1.182500	2/15/2022 2:27:29 PM
June 5m (st3) 1	2.299000	2/15/2022 12:47:32 AM
June 5m (st3) 2	2.548500	2/15/2022 12:59:03 AM
QC Deep	0.402233	2/15/2022 1:20:14 AM
Instrument blanc	-0.107967	2/15/2022 1:40:07 AM
June 5m (st3) 3	2.074000	2/15/2022 2:01:42 AM
June 30m (st3) 1	1.241500	2/15/2022 2:09:41 AM
June 30m (st3) 2	6.593000	2/15/2022 2:22:06 AM
June 30m (st3) 3	2.186000	2/15/2022 2:31:55 AM
QC surface	0.766550	2/15/2022 3:48:14 AM
Instrument blanc	-0.147933	2/15/2022 4:07:03 AM
QC mid	0.599050	2/15/2022 6:04:48 AM
Instrument blanc	-0.135367	2/15/2022 6:23:46 AM
July st3 5m 1	1.579000	2/14/2022 7:46:07 PM
July st3 5m 2	1.630000	2/14/2022 7:54:13 PM
July st3 5m 3	63.480000	2/14/2022 8:07:42 PM
July st3 30m 1	1.706000	2/14/2022 8:16:39 PM
QC surface	0.767133	2/14/2022 8:38:42 PM
Instrument blanc	-0.108200	2/14/2022 8:55:22 PM

July st3 30m 2	74.040000	2/14/2022 9:16:43 PM
July st3 30m 3	51.580000	2/14/2022 9:27:18 PM
July st1 5m 1	181.400000	2/14/2022 9:49:39 PM
July st1 5m 2	58.665000	2/14/2022 9:58:59 PM
July st1 5m 3	74.200000	2/14/2022 10:10:35 PM
July st1 30m 1	1.649500	2/14/2022 10:19:25 PM
July st1 30m 2	1.234000	2/14/2022 10:30:27 PM
July st1 30m 3	50.415000	2/14/2022 10:44:09 PM
QC mid	0.623500	2/14/2022 11:03:13 PM
Instrument blanc	-0.133467	2/14/2022 11:22:13 PM
July Blanc A1	0.863550	2/14/2022 11:40:36 PM
July Blanc A2	0.234450	2/14/2022 11:51:15 PM
July Blanc B1	119.650000	2/15/2022 12:06:32 AM
July Blanc B2	0.942800	2/15/2022 12:13:22 AM
July Blanc C1	0.142750	2/15/2022 12:24:18 AM
July Blanc C2	0.071410	2/15/2022 12:35:28 AM
MQ Blanc	-0.146750	2/14/2022 11:33:18 AM
MQ Blanc	-0.132750	2/14/2022 11:50:30 AM
Calibration curve	0.001200	2/14/2022 12:12:52 PM
Calibration curve	0.300000	2/14/2022 12:21:55 PM
Calibration curve	0.599500	2/14/2022 12:33:13 PM
Calibration curve	0.901000	2/14/2022 12:47:37 PM
Calibration curve	1.200000	2/14/2022 1:00:29 PM
QC surface	0.789700	2/14/2022 1:42:56 PM
Instrument blanc	-0.137500	2/14/2022 1:59:37 PM
Aug st3 5m 1	1.549500	3/2/2022 6:52:33 PM
Aug st3 5m 2	2.426000	2/14/2022 2:18:52 PM
Aug st3 5m 3	3.166500	2/14/2022 2:30:00 PM
Aug st3 30m 1	1.497667	2/14/2022 2:43:16 PM
Aug st3 30m 2	1.111000	2/14/2022 2:51:53 PM
Aug st3 30m 3	1.429000	2/14/2022 3:02:47 PM
QC mid	0.613933	2/14/2022 4:01:44 PM
Instrument blanc	-0.108273	2/14/2022 4:20:45 PM
QC Deep	0.469850	2/14/2022 6:18:29 PM
Instrument blanc	-0.114750	2/14/2022 6:37:52 PM
Sep st1 5m 1	2.594667	2/9/2022 1:48:10 AM

Sep st1 5m 2	2.280000	2/9/2022 1:56:18 AM
Sep st1 5m 3	1.381000	2/9/2022 2:07:42 AM
Sep st1 30m 1	2.570000	2/9/2022 2:19:01 AM
Sep st1 30m 2	3.072000	2/9/2022 2:30:16 AM
QC mid	0.555067	2/9/2022 2:51:41 AM
MQ Blanc	-0.160300	2/9/2022 3:10:35 AM
MQ Blanc	-0.176400	2/9/2022 3:27:45 AM
Sep st1 30m 3	1.582500	2/9/2022 3:46:41 AM
Sep st2 5m 1	1.285000	2/9/2022 3:57:50 AM
Sep st2 5m 2	1.723000	2/9/2022 4:11:28 AM
Sep st2 5m 3	1.578500	2/9/2022 4:19:55 AM
QC Deep	0.338233	2/9/2022 5:06:11 AM
MQ Blanc	-0.172950	2/9/2022 5:23:00 AM
MQ Blanc	-0.175100	2/9/2022 5:39:41 AM
MQ Blanc	-0.251150	2/21/2022 3:30:30 PM
QC mid	0.537467	2/21/2022 4:58:32 PM
MQ Blanc	-0.227950	2/21/2022 5:15:07 PM
QC Deep	0.340467	2/21/2022 6:54:34 PM
MQ Blanc	-0.247200	2/21/2022 7:11:10 PM
Oct St1 5m 1	2.973000	2/4/2022 6:04:24 PM
Oct St1 5m 2	1.331000	2/4/2022 6:15:17 PM
Oct St1 5m 3	2.457000	2/4/2022 6:26:29 PM
Oct St1 30m 1	3.518500	2/4/2022 6:37:38 PM
Oct St1 30m 2	2.776500	2/4/2022 6:48:51 PM
Oct St1 30m 3	1.930000	2/4/2022 7:02:05 PM
Oct St3 5m 1	1.829500	2/4/2022 7:10:25 PM
Oct St3 5m 2	1.170000	2/4/2022 7:24:56 PM
Mid seawater QC	0.697500	2/4/2022 7:47:18 PM
Blanc C	-0.180600	2/4/2022 8:04:48 PM
Blanc D	-0.197400	2/4/2022 8:18:13 PM
Oct St3 5m 3	1.771000	2/4/2022 8:37:01 PM
Oct St3 30m 1	1.756000	2/4/2022 8:48:13 PM
Oct St3 30m 3	1.595000	2/4/2022 9:12:44 PM
Oct Blanc 1	1.705500	2/4/2022 9:54:09 PM
Low Seawater QC	0.420300	2/4/2022 10:12:27 PM
Blanc E	-0.186267	2/4/2022 10:32:13 PM

Blanc D	-0.190100	2/4/2022 10:49:59 PM
Oct Blanc 2	0.384833	2/4/2022 11:10:30 PM
Oct Blanc 3	0.152250	2/4/2022 11:19:00 PM
Surface Seawater QC	0.780533	2/5/2022 12:50:48 AM
Blanc E	-0.189100	2/5/2022 1:10:57 AM
Blanc C	-0.186733	2/5/2022 1:30:49 AM
Nov St1 5m 1	2.635500	2/5/2022 3:08:41 AM
Nov St1 5m 2	1.292500	2/5/2022 3:19:47 AM
Mid Seawater QC	0.563100	2/5/2022 3:41:12 AM
Blanc A	-0.187350	2/5/2022 3:58:40 AM
low Seawater QC	0.384433	2/5/2022 4:20:13 AM
Nov St1 5m 3	5.691000	2/5/2022 4:39:35 AM
Nov St3 5m 1	46.340000	2/5/2022 4:52:02 AM
Nov St3 5m 2	38.590000	2/5/2022 5:02:50 AM
Nov St3 5m 3	1.038000	2/5/2022 5:12:31 AM
Nov St3 30m 1	1.621000	2/5/2022 5:23:17 AM
Nov St3 30m 2	2.576000	2/5/2022 5:35:00 AM
Low Seawater QC	0.381900	2/5/2022 5:53:29 AM
Blanc F	-0.175567	2/5/2022 6:13:59 AM
Blanc F	-0.190300	2/5/2022 6:31:54 AM
MQ Blanc	-0.179333	2/5/2022 12:10:58 PM
MQ Blanc	-0.175550	2/5/2022 12:28:27 PM
Surface QC	0.785333	2/5/2022 3:07:26 PM
MQ Blanc A	-0.195667	2/5/2022 3:27:05 PM
MQ Blanc B	-0.198100	2/5/2022 3:38:09 PM
Nov st1 30m 1	1.521667	3/2/2022 6:32:42 PM
Nov st1 30m 2	2.464500	3/2/2022 6:41:14 PM
Nov St1 30m 3	0.924800	2/5/2022 3:56:44 PM
Mid QC	0.596467	2/5/2022 5:38:30 PM
MQ Blanc C	-0.166350	2/5/2022 5:56:04 PM
MQ Blanc D	-0.177200	2/5/2022 6:16:22 PM
Dec St3 30m 1	0.956467	2/5/2022 6:59:51 PM
Dec St3 30m 2	1.178000	2/5/2022 7:08:19 PM
Dec St3 30m 3	1.101000	2/5/2022 7:19:45 PM
Dec St3 5m 2	1.036000	2/5/2022 7:33:08 PM
Dec St3 5m 3	1.055500	2/5/2022 7:41:24 PM

Low QC	0.410300	2/5/2022 8:11:32 PM
MQ Blanc E	-0.167700	2/5/2022 8:31:19 PM
MQ Blanc F	-0.199567	2/5/2022 8:42:25 PM

,

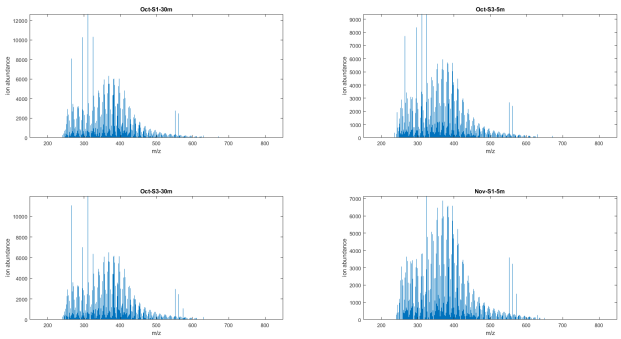

Figure 11.1: orbitrap ms spectra for the October samples and November samples. showing mass to charge ratio and ion abundance

Samplename	npeaks	totalvalue	Lipid	Unsatur	Condensed	Protein	Lignin	Tannin	Carbohydare
Sep-S1-5m	1180	1.000000e+06	383.599205	0.00000	2921.089492	4712.820458	714263.987393	114516.852334	1950.2437
Sep-S1-30m	1135	1.000000e+06	383.490849	0.00000	2314.352851	4789.840120	763462.568705	116889.747622	1084.1999
Sep-S3-5m	1139	1.000000e+06	320.647490	0.00000	5333.418243	3739.316806	792181.813647	98798.070761	608.2310
Oct-S1-5m	1124	1.000000e+06	298.165423	0.00000	6173.368330	4664.436390	734288.275738	112340.062967	1770.9992
Oct-S1-30m	1367	1.000000e+06	317.576438	0.00000	3709.551712	4242.682951	718145.831665	126098.776002	2797.7611
Oct-S3-5m	1516	1.000000e+06	304.390090	0.00000	6808.028573	4138.000444	717649.693442	126004.071696	2864.2262
Oct-S3-30m	1299	1.000000e+06	300.909906	0.00000	4414.054952	4544.774916	738043.868330	120485.300822	2059.1818
Nov-S1-5m	1410	1.000000e+06	375.555265	0.00000	3093.599407	5688.905013	750601.330967	127263.673022	2379.9282
Nov-S1-30m	1505	1.000000e+06	339.067446	0.00000	3526.471728	4793.842905	733540.495075	118146.467302	2310.6595
Nov-S3-5m	1277	1.000000e+06	377.818871	0.00000	2554.881267	5318.229042	740739.960394	112908.477061	1424.1111
Dec-S3-5m	1504	1.000000e+06	331.376123	0.00000	3346.475552	6043.317131	740094.614225	125754.911751	3272.5484
Jan-S3-5m-A	1245	1.000000e+06	346.395109	0.00000	2788.510776	5692.204123	749020.585406	131313.182710	2785.9650
Jan-S3-5m-B	1493	1.000000e+06	364.599799	0.00000	3326.501929	5496.122545	715609.576198	130489.045289	2770.4128
Jan-S3-5m-C	1434	1.000000e+06	410.426350	0.00000	2915.806480	5993.765679	728176.653879	140480.536383	3474.8353
Jan-S3-30m	1395	1.000000e+06	357.602722	0.00000	2974.059208	4865.208492	716988.574189	135310.981361	2749.9110
Feb-S3-5m	1287	1.000000e+06	365.675792	0.00000	1961.838836	4803.179291	754064.612401	125379.195814	2346.6998
Feb-S3-30m	1335	1.000000e+06	308.150541	0.00000	2404.218784	3501.991083	764873.633521	106932.965380	1446.5066
Mar-S3-5m-A	1353	1.000000e+06	428.102119	0.00000	2522.194046	5194.853249	752216.298734	112019.389060	1443.8475
Mar-S3-5m-B	1050	1.000000e+06	444.645632	0.00000	1459.806793	7386.871742	734446.031643	113500.426564	1391.2029
Mar-S3-5m-C	1232	1.000000e+06	604.946278	0.00000	921.916798	7944.904169	688935.380685	137964.319676	2777.5991
Mar-S3-30m	1133	1.000000e+06	558.683768	0.00000	1191.745939	8407.563490	682395.346672	135618.732503	2122.4427
apr-S3-5m	1605	1.000000e+06	375.323678	0.00000	3992.300498	4820.865854	742479.403123	128980.357307	2360.2989
apr-S3-30m	1314	1.000000e+06	454.196139	0.00000	2106.970755	6379.603989	737375.813870	129253.259638	1437.3718
may-S3-5m-A	1476	1.000000e+06	419.670279	0.00000	4935.289359	5964.948074	730944.458197	122321.036517	2034.0152
may-S3-5m-B	1001	1.000000e+06	576.551629	300.48901	2198.754325	8262.361807	684945.843688	124693.528368	777.6676
may-S3-5m-C	1084	1.000000e+06	382.231851	0.00000	3727.460462	7806.985934	718923.333556	119088.364159	1247.9481
may-S3-30m	1522	1.000000e+06	354.983605	0.00000	3358.128290	5237.360911	731191.197703	116673.529415	1623.2089
jun-S3-5m	1252	1.000000e+06	324.241754	0.00000	8666.697653	5389.540280	763934.486711	116965.980780	942.9594
jun-S3-30m	1240	1.000000e+06	377.948849	0.00000	2784.668078	6323.064740	752102.166597	113030.363312	541.8519
jul-S1-5m	585	1.000000e+06	661.552056	0.00000	1508.738096	14074.746983	658724.771629	139158.036926	1521.7826
jul-S1-30m	639	1.000000e+06	0.000000	0.00000	579.976825	12272.073957	796363.516963	73448.460562	451.7240
jul-S3-5m	211	1.000000e+06	0.000000	0.00000	0.000000	37765.868510	636569.006010	82148.692160	0.0000
jul-S3-30m-A	223	1.000000e+06	0.000000	0.00000	0.000000	36422.716730	742201.089590	33096.759470	0.0000
jul-S3-30m-B	543	1.000000e+06	0.000000	0.00000	1503.362653	10460.073575	793170.343897	67482.650299	472.3082
jul-S3-30m-C	581	1.000000e+06	463.438819	0.00000	386.306073	11987.465571	676305.805800	99788.313876	470.7043

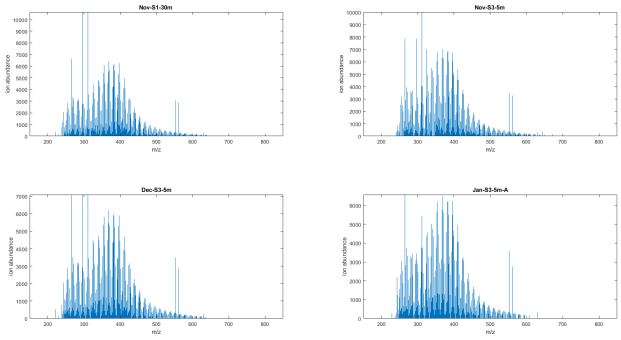

Figure 11.2: orbitrap ms spectra for the November, December samples and January samples. showing mass to charge ratio and ion abundance

Sample name	Concentration	T-test	P-value
Jan blank 1	0.00275	5.070440652399608	4.442967810620673e-05
Jan blank 1	0.05646		
Jan blank 1	0.03945		
Jan blank 2	**0.88930**		
Jan blank 2	**0.95760**		
Jan blank 2	**0.95880**		
Jan blank 3	0.22110		
Jan blank 3	0.27020		
Jan blank 3	0.27820		
Mar blank 1	0.39240	3.365146465498629	0.003250737416404648
Mar blank 1	0.41630		
Mar blank 1	0.36320		
Mar blank 2	0.25990		
Mar blank 2	0.25890		
Mar blank 3	**1.12300**		
Mar blank 3	**1.08200**		
Mar blank 3	**1.12500**		
May Blank 1	**4.18700**	-1.0937113564801866	0.29027492798521004
May Blank 1	**4.09000**		
May Blank 2	**6.09500**		
May Blank 2	**5.99400**		
May Blank 3	**5.52000**		
May Blank 3	**5.46200**		
July Blank 1	0.85770	-0.05273115910870883	0.9583652153722545
July Blank 1	0.86940		
July Blank 2	**118.90000**		
July Blank 2	**120.40000**		
July Blank 3	0.15010		
July Blank 3	0.13540		

Sample Name	concentration
Mid QC	0.5407
Mid QC	0.5118
Mid QC	0.5803
MQ Blank F	-0.1770
MQ Blank F	-0.1579
MQ Blank F	-0.1933
MQ Blank A	-0.1777
MQ Blank A	-0.1599
MQ Blank A	-0.2051
Low QC	0.4265
Low QC	0.3964
Low QC	0.3496
QC Surface	0.7712
QC Surface	0.7529
QC mid	0.6726
QC mid	0.6375
QC mid	0.6283
MQ Blank	-0.1889
MQ Blank	-0.1938
MQ Blank	-0.1805
MQ Blank	-0.1588
MQ Blank	-0.1906
QC Deep	0.4264
QC Deep	0.4063
QC Deep	0.3553
MQ Blank	-0.1741
MQ Blank	-0.1912
MQ Blank	-0.1777
MQ Blank	-0.2101
MQ Blank	-0.2089
QC Surface	0.7801
QC Surface	0.7515
QC Surface	0.7324
MQ Blank	-0.1760
MQ Blank	-0.1801
MQ Blank	-0.1620
MQ Blank	-0.1858
MQ Blank	-0.1872
QC mid	0.5914

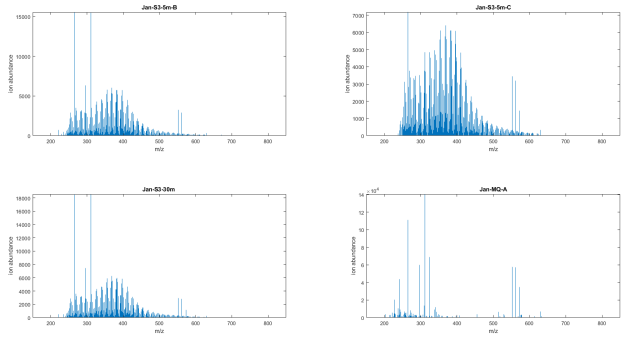

Figure 11.3: orbitrap ms spectra for the January samples and January blank samples. showing mass to charge ratio and ion abundace

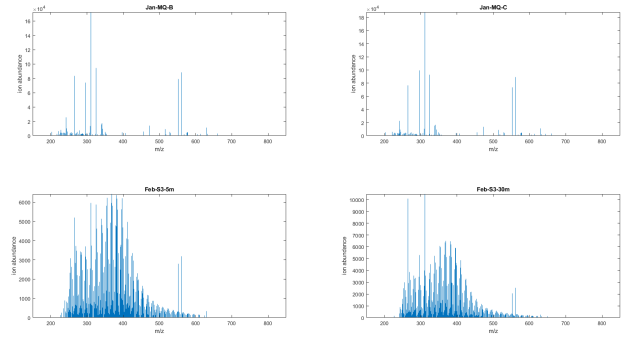

Figure 11.4: orbitrap ms spectra for the January blank samples and February samples. showing mass to charge ratio and ion abundance

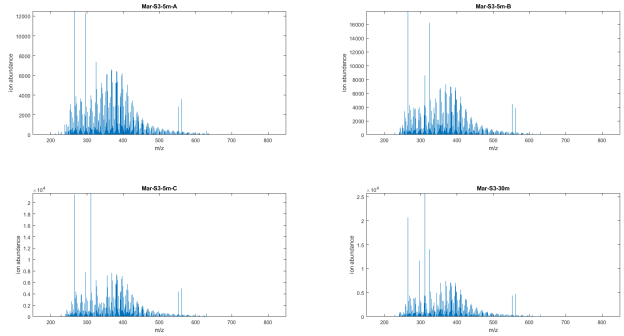

Figure 11.5: orbitrap ms spectra for the March samples. showing mass to charge ratio and ion abundance

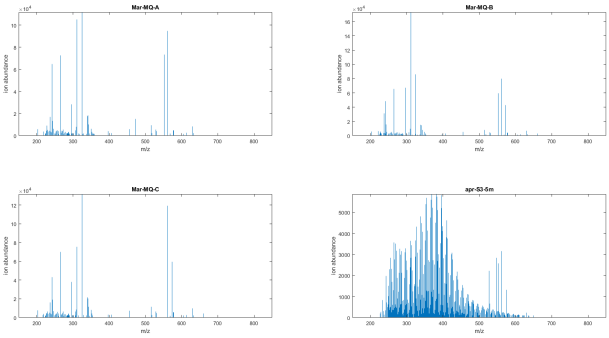

Figure 11.6: orbitrap ms spectra for the March blank samples and April samples. showing mass to charge ratio and ion abundance

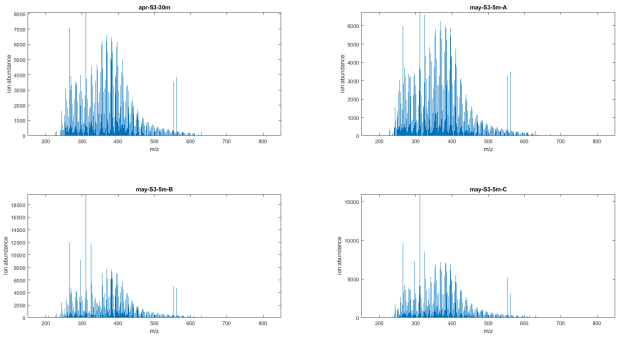

Figure 11.7: orbitrap ms spectra for the April samples and May samples. showing mass to charge ratio and ion abundance

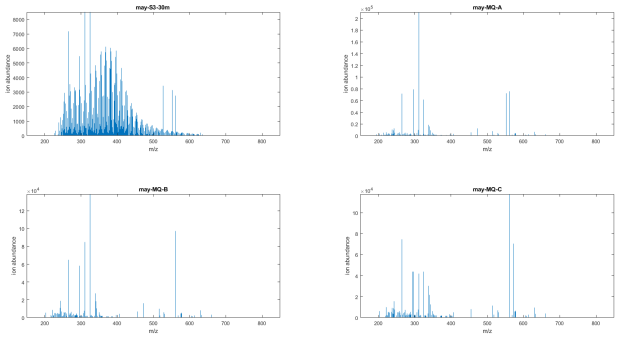

Figure 11.8: orbitrap ms spectra for the May samples and May blank samples. showing mass to charge ratio and ion abundance

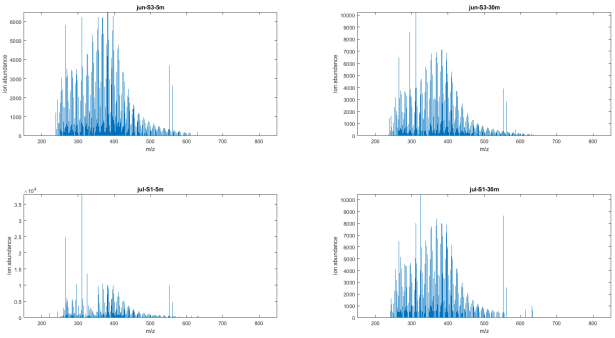

Figure 11.9: orbitrap ms spectra for the June samples and July samples. showing mass to charge ratio and ion abundance

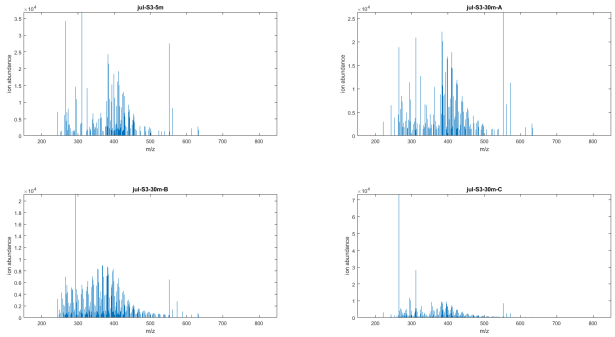

Figure 11.10: orbitrap ms spectra for the July samples. showing mass to charge ratio and ion abundance

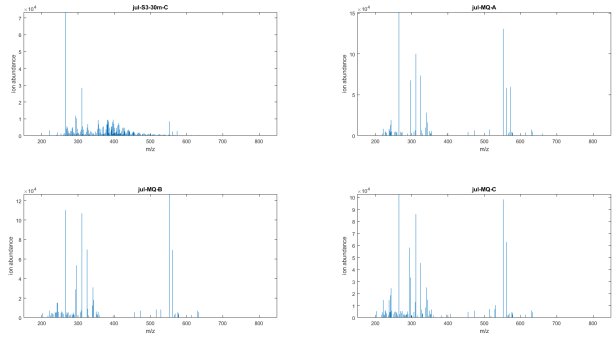

Figure 11.11: orbitrap ms spectra for the July blank samples. showing mass to charge ratio and ion abundance

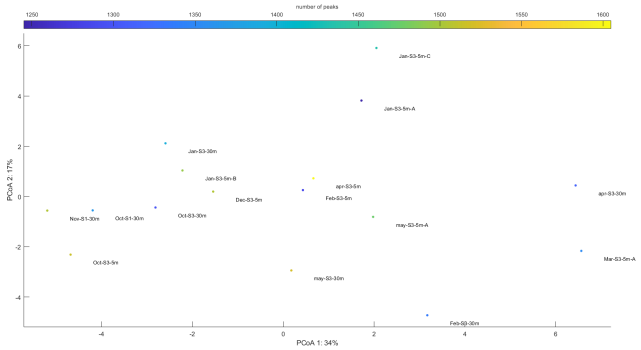

Figure 11.12: PCoA plot of all samples based on their prbitrap fingerprint data. With JunS35m, JunS330m, NovS35m, NovS15m, MayS35mC, MayS35mB, MayS330m, MarS35mB and MayS35mC removed to make it easier to look at the remaining samples.

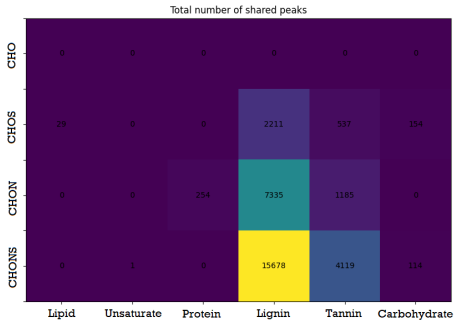

Figure 11.13: Matrix of number of shared peaks of all samples, between the compound distribution method of and the CHONS method

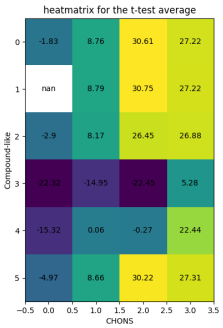

Figure 11.14: Heatmatrix of the result of T-test comparing CHONS to the compoundlike dristribution

Comp	Sum	variance	rel_variance	avg_height
Lipid	0.043790	3.192995e-08	0.000073	0.000480
Condensed aromatic	0.374798	3.822480e-06	0.001020	0.004108
Protein	0.706482	2.467880e-05	0.003493	0.007743
Lignin	76.893072	3.503357e-04	0.000456	0.842712
Tannin	13.018334	2.338829e-04	0.001797	0.142675
Carbohydrate	0.208263	9.232487e-08	0.000044	0.002282
Lipid	0.026085	3.025149e-08	0.000116	0.000320
Condensed aromatic	0.242556	2.148654e-06	0.000886	0.002976
Protein	0.575393	1.389675e-05	0.002415	0.007060
Lignin	70.170217	5.565422e-04	0.000793	0.860980
Tannin	10.330185	6.094532e-04	0.005900	0.126750
Carbohydrate	0.155965	1.218746e-06	0.000781	0.001914
Lipid	0.026745	1.726723e-08	0.000065	0.000424
Condensed aromatic	0.190124	1.638165e-06	0.000862	0.003014
Protein	0.467531	3.556623e-05	0.007607	0.007411
Lignin	53.689472	4.534877e-04	0.000845	0.851017
Tannin	8.599100	5.711568e-04	0.006642	0.136302
Carbohydrate	0.115600	7.847098e-07	0.000679	0.001832
Lipid	0.026865	1.982790e-08	0.000074	0.000417
Condensed aromatic	0.277979	6.917251e-06	0.002488	0.004312
Protein	0.469315	1.594991e-04	0.033986	0.007279
Lignin	54.715731	1.472309e-04	0.000269	0.848683
Tannin	8.839565	1.980223e-04	0.002240	0.137109
Carbohydrate	0.141860	1.324000e-06	0.000933	0.002200

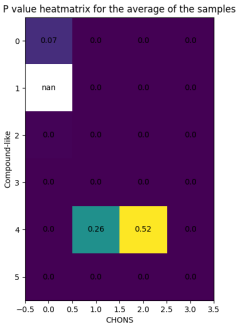

Figure 11.15: Heatmatrix of the p-value for the T-tests comparing CHONS to the compound-like dristribution

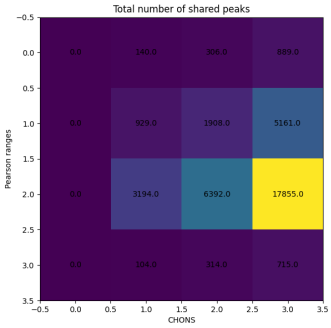

Figure 11.16: Heatmatrix of number of shared peaks between pearson ranges 1-0.6, 0.6-0, 0-(-0.6), -0.6-(-1), and distribution of compounds based on having S and N

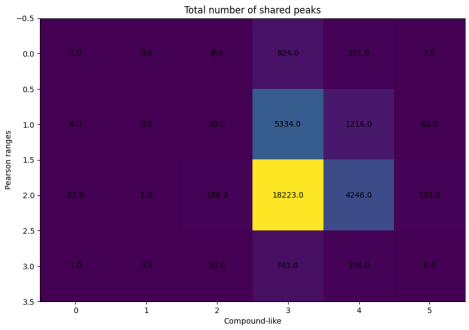

Figure 11.17: Heatmatrix of number of shared peaks between pearson ranges 1-0.6, 0.6-0, 0-(-0.6), -0.6-(-1), and distribution of compounds based on "compound-likeness"